**1 Holocene aridification trend interrupted by millennial- and centennial-scale climate**
**2 fluctuations from a new sedimentary record from Padul (Sierra Nevada, southern Iberian**
**3 Peninsula)**

4 María J. Ramos-Román[1], Gonzalo Jiménez-Moreno[1], Jon Camuera[1], Antonio García-Alix[1], R.
5 Scott Anderson[2], Francisco J. Jiménez-Espejo[3], José S. Carrión[4]

6 [1] Departamento de Estratigrafía y Paleontología, Universidad de Granada, Spain
7 [2] School of Earth Sciences and Environmental Sustainability, Northern Arizona University,
8 USA.
9 [3] Department of Biogeochemistry, Japan Agency for Marine-Earth Science and Technology
10 (JAMSTEC), Japan.
11 [4] Departamento de Biología Vegetal, Facultad de Biología, Universidad de Murcia, Murcia,
12 Spain.

13 *Correspondence to:* María J. Ramos-Román (mjrr@ugr.es)

14 **Abstract.** Holocene centennial-scale paleoenvironmental variability has been described in a
15 multiproxy analysis (i.e. lithology, geochemistry, macrofossil and microfossil analyses) of a
16 paleoecological record from the Padul basin in Sierra Nevada, southern Iberian Peninsula. This
17 sequence covers a relevant time interval hitherto unreported in the studies of the Padul
18 sedimentary sequence. The ca. 4700 yr-long record has preserved proxies of climate variability,
19 with vegetation, lake levels and sedimentological change the Holocene in one of the most unique
20 and southernmost peat bogs from Europe. The progressive Middle and Late Holocene trend
21 toward arid conditions identified by numerous authors in the western Mediterranean region,
22 mostly related to a decrease in summer insolation, is also documented in this record, being here
23 also superimposed by centennial-scale variability in humidity. In turn, this record shows
24 centennial-scale climate oscillations in temperature that correlate with well-known climatic
25 events during the Late Holocene in the western Mediterranean region, synchronous with
26 variability in solar and atmospheric dynamics. The multiproxy Padul record first shows a
27 transition from a relatively humid Middle Holocene in the western Mediterranean region to more
28 aridity from ~4700 to ~2800 cal yr BP. A relatively warm and humid period occurred between
29 ~2600 to ~1600 cal yr BP, coinciding with persistent negative NAO conditions and the historic
30 Iberian-Roman Humid Period. Enhanced arid conditions, co-occurring with overall positive
31 NAO conditions and increasing solar activity, are observed between ~1550 to ~ 450 cal yr BP
32 (~400 to ~1400 CE) and colder and warmer conditions happened during the Dark Ages and
33 Medieval Climate Anomaly, respectively. Slightly wetter conditions took place during the end of
34 the MCA and the first part of the Little Ice Age, which could be related to a change towards
35 negative NAO conditions and minima in solar activity. Evidences of higher human impact in the
36 Padul peat bog area are observed in the last ~1550 cal yr BP. Time series analysis performed
37 from local (*Botryococcus* and TOC) and regional signals (Mediterranean forest) helped us
38 determining the relationship between southern Iberian climate evolution, atmospheric, oceanic
39 dynamics and solar activity.

40 **Keywords:** Holocene, Padul**,** peat bog, North Atlantic Oscillation, atmospheric dynamics,
41 southern Iberian Peninsula, Sierra Nevada, western Mediterranean.

## 1  Introduction

The Mediterranean area is situated in a sensitive region between temperate and subtropical climates making it an important place to study the connections between atmospheric and oceanic dynamics and environmental changes. Climate in the western Mediterranean and the southern Iberian Peninsula is influenced by several atmospheric and oceanic dynamics (Alpert et al., 2006), including the North Atlantic Oscillation (NAO) one of the principal atmospheric phenomenon controlling climate in the area (Hurrell, 1995; Moreno et al., 2005). Recent NAO reconstructions in the western Mediterranean region relate negative and positive NAO conditions with an increase and decrease in winter (effective) precipitation, respectively (e.g. Olsen et al., 2012; Trouet et al., 2009). Numerous paleoenvironmental studies in the western Mediterranean have detected a link at millennial- and centennial-scales between the oscillations of paleoclimate proxies studied in sedimentary records with solar variability and atmospheric (i.e., NAO) and/or ocean dynamics during the Holocene (e.g. Fletcher et al., 2013; Moreno et al., 2012; Rodrigo-Gámiz et al., 2014). Very few montane and low altitude lake records in southern Iberia document centennial-scale climate change [see, for example Zoñar Lake (Martín-Puertas et al., 2008)], with most terrestrial records in the western Mediterranean region evidencing only millennial-scale cyclical changes. Therefore, higher-resolution decadal-scale analyses are thus necessary in order to analyze the link between solar activity, atmospheric and oceanographic systems with terrestrial environment in this area at shorter (ie., centennial) time scales.

Sediments from lakes, peat bogs and marine records from the western Mediterranean have documented an aridification trend during the Late Holocene (e.g. Carrión et al., 2010b; Gil-Romera et al., 2014; Jalut et al., 2009). This trend, however, was superimposed by shorter-term climate variability, as shown by several recent studies from the region, as well as human pressure (Carrión, 2002; Fletcher et al., 2013; Jiménez-Moreno et al., 2013; Martín-Puertas et al., 2008; Ramos-Román et al., 2016). This relationship between climate variability, culture evolution and human impact during the Late Holocene has also been the subject of recent paleoenvironmental studies (Carrión et al., 2007; Lillios et al., 2016; López-Sáez et al., 2014; Magny, 2004). However, it is still unclear what has been the main forcing driving environmental change (i.e., deforestation) in this area during this time: was it climate or humans?

Within the western Mediterranean region, Sierra Nevada is the highest and southernmost mountain range in the Iberian Peninsula and thus presents a critical area for paleoenvironmental studies. Most high-resolution studies there have come from high elevation sites. The well-known Padul peat bog site is located at the western foot of the Sierra Nevadas (Fig. 1) and bears one of the longest continental records in southern Europe, with a sedimentary sequence of ca. 100 m thick that could represent the last 1 Ma  (Ortiz et al., 2004). Several research studies, including radiocarbon dating, geochemistry and pollen analyses, have been carried out on previous cores from Padul, and have documented glacial/interglacial cycles during the Pleistocene and up until the Middle Holocene. However, the Late Holocene section of the Padul sedimentary sequence has never been retrieved and studied. This was due to the location of these previous corings within the peat mine exploitation setting, where the upper (and non productive) part of the sedimentary sequence was missing (Florschütz et al., 1971; Ortiz et al., 2004; Pons and Reille, 1988).

Here we present a new record from the Padul peat bog basin: Padul-15-05, a 42.64 m-long sediment core that, for the first time, contains a continuous record of the Late Holocene (Fig. 2). A high-resolution multi-proxy analysis of the upper 1.15 m, the past ~4700 cal yr BP, has allowed us to determine a complete paleoenvironmental and paleoclimatic record at centennial-

88   and millennial-scales. To accomplish that, we reconstructed changes in the Padul peat bog
89   vegetation, sedimentation, climate and human impact during the Holocene throughout the
90   interpretation of the lithology, palynology and geochemistry.

91   Specifically, the main objective of this paper is to determine environmental variability and
92   climate evolution in the southern Iberian Peninsula and the western Mediterranean region and
93   their linkages to northern hemisphere climate and solar variability during the Holocene. In order
94   to do this, we compared our results with other paleoclimate records from regional areas and solar
95   activity from the northern hemisphere for the past ca. 4.7 cal ka BP (Bond et al., 2001; Laskar et
96   al., 2004; Sicre et al., 2016; Steinhilber et al., 2009).

## 97   2   Study site

### 98   2.1 Regional setting: Sierra Nevada climate and vegetation

99   Sierra Nevada is a W-E aligned mountain range located in Andalusia (southern Spain). Climate
100  in this area is Mediterranean, with cool and humid winters and hot/warm summer drought. In the
101  Sierra Nevada, the mean annual temperature at approximately 2500 m asl is 4.5 ºC and the mean
102  annual precipitation is 700 mm/yr (Oliva et al., 2009). Sierra Nevada is strongly influenced by
103  thermal and precipitation variations due to the altitudinal gradient (from ca. 700 to more than
104  3400 m), which control plant taxa distribution in different bioclimatic vegetation belts due to the
105  variability in thermotypes and ombrotypes (Valle Tendero, 2004). According to the
106  climatophilous series classification, Sierra Nevada is divided in four different vegetation belts
107  (Fig. 1). The crioromediterranean vegetation belt, occurring above ~2800 m, is characterized
108  principally by *Festuca clementei*, *Hormatophylla purpurea*, *Erigeron frigidus*, *Saxifraga*
109  *nevadensis*, *Viola crassiuscula*, and *Linaria glacialis*. The oromediterranean belt, between ~1900
110  to 2800 m, bears *Pinus sylvestris*, *P. nigra*, *Juniperus communis subsp. hemisphaerica*, *J. sabina*
111  var. *humilis*, *J. communis* subsp. *nana*, *Genista versicolor*, *Cytisus oromediterraneus*,
112  *Hormatophylla spinosa*, *Prunus prostrata*, *Deschampsia iberica* and *Astragalus sempervirens*
113  subsp. *nevadensis* as the most representative species. The supramediterranean belt, from
114  approximately 1400 to 1900 m of elevation, principally includes *Quercus pyrenaica*, *Q. faginea*,
115  *Q. rotundifolia*, *Acer opalus* subsp. *granatense*, *Fraxinus angustifolia*, *Sorbus torminalis*,
116  *Adenocarpus decorticans*, *Helleborus foetidus*, *Daphne gnidium*, *Clematis flammula*, *Cistus*
117  *laurifolius*, *Berberis hispanicus*, *Festuca scariosa*, *Thymus serpylloides* subsp. *gadoriensis*,
118  *Helichrysum italicum* subsp. *serotinum*, *Santolina rosmarinifolia* subps. *canescens* and *Artemisia*
119  *glutinosa*. The mesomediterranean vegetation belt occurs between ~600 and 1400 m of elevation
120  and is characterized by *Quercus rotundifolia*, *Retama sphaerocarpa*, *Paeonia coriacea*,
121  *Juniperus oxycedrus*, *Rubia peregrina*, *Asparagus acutifolius*, *D. gnidium*, *Ulex parviflorus*,
122  *Genista umbellata*, *Cistus albidus* and *C. lauriflolius* (Al Aallali et al., 1998; Valle, 2003). The
123  human impact over this area, especially important during the last millennium, affected the
124  natural vegetation distribution through fire, deforestation, cultivation. (i.e., *Olea*) and subsequent
125  reforestation (mostly *Pinus)* (Anderson et al., 2011).

### 126  2.2 Padul peat bog

127  The Padul basin is situated at approximately 725 m of elevation in the southeastern part of the
128  Granada Basin, at the foothill of the southwestern Sierra Nevada, Andalucía, Spain (Fig. 1). This
129  is one of the most seismically active areas in the southern Iberian Peninsula with numerous faults

130   in NW-SE direction, with the Padul fault being one of these active normal faults (Alfaro et al.,
131   2001). It is a small extensional basin approximately 12 km long and covering an area of
132   approximately 45 km$^2$, which is bounded by the Padul normal fault. The sedimentary in-filling of
133   the basin consists of Neogene and Quaternary deposits; Upper Miocene conglomerates,
134   calcarenites and marls, and Pliocene and Quaternary alluvial sediments, lacustrine and peat bog
135   deposits (Sanz de Galdeano et al., 1998; Delgado et al., 2002; Domingo et al., 1983). The Padul
136   peat bog is an endorheic area with a surface of approximately 4 km$^2$ placed in the Padul basin
137   that contains a sedimentary sequence mostly characterized by peat. The basin fill is asymmetric,
138   with thicker peat infill to the northeast (~100 m thick; Domingo-García et al., 1983; Florschütz et
139   al., 1971; Nestares and Torres, 1997) and disappearing to the southwest (Alfaro et al., 2001). The
140   main source area of the sediments in the Padul peat bog is Sierra Nevada, which is characterized
141   at higher elevations by Paleozoic siliceous metamorphic rocks (mostly mica-schists and
142   quartzites) from the Nevado-Filabride complex and, at lower elevations and acting as bedrock,
143   by Triassic dolomites, limestones and phyllites from the Alpujárride Complex (Sanz de
144   Galdeano et al. 1998). Geochemistry in the Padul sediments is influenced by detritic materials
145   coming from the neighboring mountains, mainly the Sierra Nevada mountain range (Ortiz et al.,
146   2004). In addition, groundwater inputs into the Padul basin are the main reason why there is a
147   wetland in this area. These inputs come from the Triasic carbonates aquifers (N and S edge to the
148   basin), the out flow of the Granada Basin (W) and the conglomerate aquifer to the east edge
149   (Castillo Martín et al., 1984; Ortiz et al., 2004). The main water output is by evaporation and
150   evapotranspiration, water wells and by canals ("madres") that drain the water to the Dúrcal river
151   to the southeast (Castillo Martín et al., 1984). Climate in the Padul area is characterized by a
152   mean annual temperature of 14.4 ºC and a mean annual precipitation of 445 mm
153   (http://www.aemet.es/).
154   Vegetation in the Padul area is dominated by *Q. rotundifolia* (and in less amounts *Q. faginea*),
155   which is normally accompanied by *Pistacia terebinthus*. Shrub species in the area include
156   *Juniperus oxycedrus*, *Crataegus monogyna*, *Daphne gnidium* and *Ruscus aculeatus*. Creepers
157   such as *Lonicera implexa*, *Rubia peregrina*, *Hedera helix*, *Asparagus acutifolius* also occur in
158   this area and some herbs, such as *Paeonia broteroi*. *Quercus coccifera* also occurs in crests and
159   very sunny rocky outcrops. *Retama sphaerocarpa* and *Genista cinerea* subsp. *speciosa* and the
160   *Thymo-Stipetum tenacissime* series also occur in sunny areas and in more xeric soils.
161   Nitrophilous communities occur in soils disrupted by livestock, pathways or open forest,
162   normally related with anthropization (Valle, 2003).
163   The Padul-15-05 drilling site was located around 50 m south of the present-day Padul lake shore
164   area. This basin area is presently subjected to seasonal water level fluctuations and is principally
165   dominated by *Phragmites australis* (Poaceae). The lake environment is dominated by aquatic
166   and wetland communities with *Chara vulgaris*, *Myriophyllum spicatum, Potamogeton
167   pectinatus, Potamogetum coloratus*, *Phragmites australis, Typha dominguensis*, *Apium
168   nodiflorum*, *Juncus subnodulosus, Carex hispida, Juncus bufonius* and *Ranunculus muricatus*
169   between others (Pérez Raya and López Nieto, 1991). Some sparse riparian trees occur in the
170   northern lake shore, such as *Populus alba*, *Populus nigra*, *Salix* sp., *Ulmus minor* and *Tamarix*.

171   **3 Material and methods**

172   Two sediment cores, Padul-13-01 (37º00'40''N; 3º36'13''W) and Padul-15-05 (37º00'39.77''N;
173   3º36'14.06''W) with a length of 58.7 cm and 42.64 m, respectively, were collected between
174   2013 and 2015 from the peat bog (Fig. 1). The cores were taken using a Rolatec RL-48-L drilling

175  machine equipped with a hydraulic piston corer from the Scientific Instrumentation Centre of the
176  University of Granada. The sediment cores were wrapped in film, put in core boxes, transported
177  and stored in a dark cool room at +4ºC.

**3.1 Age-depth model (AMS radiocarbon dating)**

179  The core chronology was constrained using fourteen AMS radiocarbon dates from plant remains
180  and organic bulk samples taken throughout the cores (Table 1). In addition, one sample with
181  gastropods was also measured for AMS radiocarbon analysis, although it was rejected due to
182  important reservoir effect, which provide a very old date. Thirteen of these samples came from
183  Padul-15-05 and one from the nearby Padul-13-01 (Table 1). We were able to use this date from
184  Padul-13-01 core as there is a very significant correlation between the upper part of Padul-15-05
185  and Padul-13-01 cores, shown by identical lithological and geochemical changes (Supplementary
186  information 1; Figure S1). The age model for the upper ~3 m until 21 cm from the surface was
187  built using the R-code package 'Clam 2.2' (Blaauw, 2010) employing the calibration curve
188  IntCal 13 (Reimer et al., 2013), a 95 % of confidence range, a smooth spline (type 4) with a 0.20
189  smoothing value and 1000 iterations (Fig. 2). The chronology of the uppermost 21 cm of the
190  record was built using a lineal interpolation between the last radiocarbon date and the top of the
191  record (Present; 2015 CE). The studied interval in the present work are the uppermost 115 cm of
192  the record that are constrained by six AMS radiocarbon dates (Fig. 2).

**3.2 Lithology, MS, XRF and TOC**

194  The length for the Padul-15-05 core is ~ 43 m. In this study, we focus in the uppermost ~ 115 cm
195  from that core. Padul-15-05 core was split longitudinally and was described in the laboratory
196  with respect to lithology and color (Fig. 3).
197  Magnetic susceptibility (MS) was measured with a Bartington MS3 operating with a MS2E
198  sensor. MS measurements (in SI units) were obtained directly from the core surface every 0.5 cm
199  (Fig. 3).
200  Elemental geochemical composition was measured in an X-Ray fluorescence (XRF) Avaatech
201  core scanner® at the University of Barcelona (Spain). A total of thirty-three chemical elements
202  were measured in the XRF core scanner at 10 mm of spatial resolution, using 10 s count time, 10
203  kV X-ray voltage and a X-ray current of 650 μA for lighter elements and 35 s count time, 30 kV
204  X-ray voltage, X-ray current of 1700 μA for heavier elements. Thirty-three chemical elements
205  were measured but only the most representative with a major number of counts were considered
206  (Si, K, Ca, Ti, Fe, Zr, Br and Sr). Results for each element are expressed as intensities in counts
207  per second (cps) and normalized (norm.) for the total sum in cps in every measure (Fig. 3).
208  Total organic carbon (TOC) was analyzed every 2 or 3 cm throughout the core. Samples were
209  previously decalcified with 1:1 HCl in order to eliminate the carbonate fraction. The percentage
210  of organic Carbon (OC %) was measured in an Elemental Analyzer Thermo Scientific Flash
211  2000 model from the Scientific Instrumentation Centre of the University of Granada (Spain).
212  Percentage of TOC per gram of sediment was calculated from the percentage of organic carbon
213  (OC %) yielded by the elemental analyzer, and recalculated by the weight of the sample prior to
214  decalcification (Fig. 3).

**3.3 Pollen and NPP**

216  Samples for pollen analysis (1-3 cm³) were taken every 1 cm throughout the core. Pollen
217  extraction methods followed a modified Faegri and Iversen (1989) methodology. Processing
218  included the addition of *Lycopodium* spores for calculation of pollen concentration. Sediment
219  was treated with NaOH, HCl, HF and the residue was sieved at 250 mm previous to an acetolysis
220  solution. Counting was performed using a transmitted light microscope at 400 magnifications to
221  an average pollen count of ca. 260 terrestrial pollen grains. Fossil pollen was identified using
222  published keys (Beug, 1961) and modern reference collections at University of Granada (Spain).
223  Pollen counts were transformed to pollen percentages based on the terrestrial pollen sum,
224  excluding aquatics. The palynological zonation was executed by cluster analysis using twelve
225  different pollen taxa- *Olea*, *Pinus* undifferentiated, deciduous *Quercus*, evergreen *Quercus*,
226  *Pistacia*, Ericaceae, *Artemisia*, Asteroideae, Cichorioideae, Amaranthaceae and Poaceae
227  (Grimm, 1987) (Fig. 4). Non-pollen palynomorphs (NPP) include fungal and algal spores, and
228  thecamoebians (testate amoebae). The NPP percentages were calculated and represented with
229  respect to the terrestrial pollen sum (Fig. 4). Furthermore, some pollen taxa were grouped,
230  according to present-day ecological bases, in Mediterranean forest and xerophytes (Fig. 4). The
231  Mediterranean forest taxa is composed of *Quercus* total, *Olea*, *Phillyrea* and *Pistacia*. The
232  xerophyte group includes *Artemisia*, *Ephedra*, and Amaranthaceae.

## 233  4 Results

### 234  4.1 Chronology and sedimentation rates

235  The age-model of the studied Padul-15-05 core (Fig. 2) shows that the top 115 cm continuously
236  cover approximately the last ca. 4700 cal yr BP, being the age constrained by fourteen AMS [14]C
237  dates (Table 1). Five distinct sediment accumulation rate (SAR) intervals can be differentiated
238  between 0 and 122.96 cm based on the linear interpolation between radiocarbon dates in the
239  studied core (Fig. 2).

### 240  4.2 Lithology, MS, XRF and TOC

241  The lithology of the upper ca. 115 cm of the Padul-15-05 sediment core was mainly deduced
242  from a visual inspection together with the element geochemical composition (XRF) and the
243  correlation of these data, and the MS of the split cores. In addition, this information was
244  complemented with the TOC (Fig. 3).
245  A Linear r (Pearson) correlation was calculated for the XRF data, the correlation for the
246  inorganic geochemical elements show us two different groups of elements that covary (Table 2):
247  Group 1) Si, K, Ti, Fe and Zr with a high positive correlation between them; Group 2) Ca, Br
248  and Sr have negative correlation with Group 1. The lithology for this sedimentary sequence
249  consists in clays with variable carbonates, siliciclastics and organic content (Fig. 3). Based on
250  this, the sequence is subdivided in two principal sedimentary units. The bottom of the record
251  corresponds with Unit 1, characterized principally by lower values of MS and higher values of
252  Ca. The top of the sequence can be subdivided in Unit 2, in which the mineralogical composition
253  is lower in Ca with higher values of MS in correlation with mostly siliciclastics elements (Si, K,
254  Ti, Fe and Zr). Within these two units, four different facies can be identified by visual inspection
255  and by the elemental geochemical composition and TOC of the sediments. *Facies* 1, between
256  115-110 cm depth (ca. 4700 to 4650 cal yr BP) and 89-80 cm depth (ca. 4300 to 4000 cal yr BP),
257  are characterized by dark brown organic clays that bear charophytes and plant remains. They are

258   also depicted by relative higher values of TOC values (Fig. 3). *Facies* 2, between 110-89 cm
259   depth (ca. 4650 to 4300 cal yr BP) and 80-42 cm depth (ca. 4000 to 1600 cal yr BP), are made up
260   of brown clays, with the occurrence of gastropods and charophytes. These are also characterized
261   with decreasing TOC values. *Facies* 3, between 42-28 cm depth (ca. 1600 to 450 cal yr BP), are
262   characterized by grayish brown clays with the occurrence of gastropods, and lower values of
263   TOC, the increasing trend in MS and in siliciclastic elements. *Facies* 4, between 28-0 cm/ ca.
264   450 cal yr BP to Present, are made up of light grayish brown clays and feature a strong increase
265   in siliciclastic linked to a strong increase in MS.

266   **4.3 Pollen and NPP**

267   A total of seventy-two pollen taxa were identified but only the most representative taxa are here
268   plotted in a summary pollen diagram (Fig. 4). Selected NPP percentages are also displayed in
269   Figure 4. Four pollen zones (Fig. 4) were visually identified with the help of a cluster analysis
270   using the program CONISS (Grimm, 1987). Pollen zones are described below:

271   **4.3.1 Zone Padul-15-05-1 [~4720 to 3400 cal yr BP/ ~2800 to 1450 BCE (115-65 cm)]**

272   Zone 1 is characterized by the abundance of Mediterranean forest species reaching up to ca. 70
273   %. Another important taxon in this zone is *Pinus,* with average values around 18 %. Herbs are
274   largely represented by Poaceae, averaging around 10 %, and reaching up to ca. 25 %. This pollen
275   zone is subdivided into subzones-1a, 1b and 1c (Fig. 4). The principal characteristic that
276   differentiate subzone-1a to subzone-1b (boundary at ca. 4650 cal yr BP/ca. 2700 BCE) is the
277   decrease in Poaceae from an average value of ca. 18 to 10 %, the increase in *Pinus* from ca. 7 to
278   18 %, and the appearance of cf. *Vitis.* The decrease in Mediterranean forest to average values
279   around 40 %, the increase in *Pinus* to average values around 25 % and a progressive increase in
280   Ericaceae with average occurrences from ca. 6 to 11 %, allow to discern subzones 1b and 1c
281   (boundary at ca. 3950 cal yr BP).

282   **4.3.2. Zone Padul-15-05-2 [~3400 to 1550 cal yr BP/~1450 BCE to 400 CE (65-41 cm)]**

283   The main features of this zone are the increase in Ericaceae up to ca. 16 % and in deciduous
284   *Quercus*, reaching values around 20 %. Therefore, the Mediterranean forest component
285   progressively decreased to values around 34 %. Some herbs such as Cichorioideae became more
286   abundant reaching average occurrences around 7 %. This pollen zone can be subdivided in
287   subzones 2a and 2b with a boundary at ~2850 cal yr BP (~900 BCE). The principal
288   characteristics that differentiate these subzones is marked by the increase in Mediterranean forest
289   types and the increasing trend in deciduous *Quercus* and Ericaceae. The increase in
290   *Botryococcus* averages ca. 4 to 9 % and the expansion of *Mougeotia and Zygnema* type are also
291   noticeable.

292   **4.3.3 Zone Padul-15-05-3 [~1550 to 450 cal yr BP/~400 CE to 1500 CE (41-29 cm)]**

293   This zone is distinguished by the maximum depletion of Mediterranean forest elements.
294   Cichorioideae reached average values of about 40 %. The decrease in Ericaceae is also
295   significant. A decrease in *Botryococcus* and other algal remains is observed in this zone,
296   although there is an increase in other Thecamoebians from average values <1 % to 10 %. This
297   pollen zone is subdivided in subzones 3a and 3b at ~1000 cal yr BP (~950 CE). The main

298 features that differentiate these subzones are the increase in *Olea* from subzone 3a to 3b from
299 average values of ca. 1 to 5 %. The increasing trend in Poaceae is also a feature in this subzone,
300 as well as the slight increase in Asteroideae at the top. Significant changes are documented in
301 NPP percentages in this subzone with the expansion of some fungal remain such as *Tilletia* and
302 *Glomus* type. Furthermore, a decrease in *Botrycoccus* and the near disappearance of other algal
303 remains such as *Mougetia* occurred.

### 4.3.4 Zone Padul-15-05-4 [~last 450 cal yr BP/ ~ 1500 CE to Present (29-0 cm)]

305 The main feature in this zone is the significant increase in *Pinus,* reaching maximum values (ca.
306 32 %), an increase in Poaceae (ca. 40 %) and the decrease in Cichorioideae (from average
307 occurrences of ca. 44 to 16 %). Other important changes are the nearly total disappearance of
308 some shrubs such as *Pistacia* and a decreasing trend in Ericaceae, as well as an important
309 decrease in Mediterranean forest pollen. An increase in wetland pollen taxa, mostly *Typha* also
310 occurred. A significant increase in xerophytes, with the expansion of Amaranthaceae to ~14 %,
311 is also observed in this period. Other herbs such as *Plantago*, Polygonaceae and Convolvulaceae
312 show moderate increases. This zone 4 is subdivided into subzones 4a and 4b (Fig. 4). The top of
313 the record, which corresponds approximately 1830 CE to Present, is characterized by the
314 subzone 4b, the main characteristic that differentiate subzone 4b from the previous 4a is a
315 decrease in some herbs such as Cichorioideae. However, an increase in some xerophytic herbs
316 such as Amaranthaceae occurred. The increase in *Plantago* is also significant during this period.
317 A noteworthy increase in *Pinus* (from an average of ca. 14 to 27 %) and a slight increase in *Olea*
318 and evergreen *Quercus* are also characteristic of this subzone. With respect to NPP, there is an
319 increase in thecamoebians such as *Arcella* type and in the largely coprophilous sordariaceous
320 (Sordariales) group. This zone also documents the decrease in fresh-water algal spores, in
321 *Botryococcus* concomitant with *Mougeotia and Zygnema type*.

### 4.4 Estimated lake level reconstruction

323 Different local proxies from the Padul-15-05 record [Si, Ca, TOC, MS, Hygrophytes (made up of
324 Cyperaceae and Typha), Poaceae and Algae (including Botryoccocus, Zygnema type
325 and Mougeotia) groups] have been depicted in order to understand the relationship between
326 lithological, geochemical, and palynological variability and the water lake level oscillations.
327 Sediments with higher values of TOC (more algae and hygrophytes), rich in Ca (related with the
328 occurrence of shells and charophytes remains) most likely characterized a shallow water
329 environment. The absence of aquatic shells, decreasing Ca and a lower TOC and/or a higher
330 input of clastic material (higher MS and Si values) into the lake, could be related with lake level
331 lowering, and a shallower wetland environment (increase in Poaceae) (Fig. 5).

### 4.5 Spectral analysis

333 Spectral analysis was performed on selected pollen and NPP time series (Mediterranean forest
334 and *Botryococcus)*, as well as TOC in order to identify millennial- and centennial-scale
335 periodicities in the Padul-15-05 record. The mean sampling resolution for pollen and NPP is ca.
336 50 yr and for geochemical data is ca. 80 yr. Statistically significant cycles, above the 90, 95 and
337 99 % of confident levels, were found around 800, 680, 300, 240, 200, 170 (Fig. 7).

## 5 Discussion

Different proxies have been used in this study to interpret the paleoenvironmental and hydrodynamic changes recorded in the Padul peat bog sedimentary record during the last 4700 cal yr BP. Palynological analysis (pollen and NPP) is commonly used as a proxy for climate change, lake level variations and human impact and land uses (e.g. Faegri and Iversen, 1990; van Geel et al., 1983). In this study, we used the variations between Mediterranean forest taxa, xerophytes and algal communities for paleoclimatic variability and the occurrence of nitrophilous and ruderal plant communities and some NPPs for identifying human influence in the study area (Fig. 4). Variations in arboreal pollen (AP, including Mediterranean tree species) have previously been used in the Sierra Nevada records as a proxy for humidity changes (Jiménez-Moreno and Anderson, 2012; Ramos-Román et al., 2016). The abundance of the Mediterranean forest has been used as a proxy for climate change in other studies in the western Mediterranean region, with higher forest development generally meaning higher humidity (Fletcher et al., 2013; Fletcher and Sánchez-Goñi, 2008). On the other hand, increases in xerophyte pollen taxa (i.e., *Artemisia*, *Ephedra*, Amaranthaceae) have been used as an indication of aridity in this area (Anderson et al., 2011; Carrión et al., 2007).

The chlorophyceae alga *Botryococcus* sp. has been described as an indicator of freshwater environments, in relatively productive fens, temporary pools, ponds or lakes (Guy-Ohlson, 1992). The high visual and statistical correlation between *Botryococcus* from Padul-15-05 and North Atlantic temperature estimations (Bond et al., 2001; r = -0.63; *p* < 0.0001; between ca. 4700 to 1500 cal ka BP – the decreasing and very low *Botryococcus* occurrence in the last 1500 cal yr BP makes this correlation moderate: r=-0.48; *p* < 0.0001 between 4700 and -65 cal yr BP) seems to show that in this case *Botryococcus* is driven by temperature change and would reflect variations in lake productivity (increasing with warmer water temperatures).

In addition to the palynological analysis, variations in the lithology, geochemistry and macrofossil remains (gastropod shells and charophytes) from the Padul-15-05 core helped us reconstruct the estimated lake level and the local environment changes in the Padul peat bog. Several previous studies on Late Holocene lake records from the Iberian Peninsula show that lithological changes can be used as a proxy for lake level reconstruction (Martín-Puertas et al., 2011; Morellón et al., 2009; Riera et al., 2004). For example, carbonate sediments formed by biogenic remains of gastropods and charophytes are indicative of shallow lake waters (Riera et al., 2004). Furthermore, van Geel et al. (1983), described occurrences of *Mougeotia* and *Zygnema* type (Zygnemataceae) as typical of shallow water environments. The increase in organic matter accumulation deduced by TOC (and Br) could be considered as characteristic of high productivity (Kalugin et al., 2007) in these shallow water environments. On the other hand, increases in clastic input in lake sediments have been interpreted as due to lowering of lake level and more influence of terrestrial-fluvial deposition in a very shallow/ephemeral lake (Martín-Puertas et al., 2008). We used the variations between those proxies to estimate water level (Fig. 5).

Nitrophilous and ruderal pollen taxa (*Convolvulus*, *Plantago lanceolata* type, Urticaceae type and/or *Polygonum avicularis* type) are also very useful as proxies for human impact (Riera et al., 2004). Some species of Cichorioideae have also been described in different studies from the Iberian Peninsula as nitrophilous taxa (Abel-Schaad and López-Sáez, 2013). At the same time, NPP taxa such as some coprophilous fungi, Sordariales and thecamoebians are also used as indicators of anthropization and land use (Carrión et al., 2007; Ejarque et al., 2015; van Geel et al., 1989; Riera et al., 2006). *Tilletia* a grass-parasitizing fungi has been described as an indicator

384    of grass cultivation in other Iberian records (Carrión et al., 2001b). In this study we also used the
385    NPP mycorrhizal fungus *Glomus* sp. as a proxy for erosive activity. This interpretation comes
386    from a study from van Geel et al. (1989), who correlated erosive events with elevated
387    percentages of *Glomus* cf. *fasciculatum*.

388    **5.1 Late Holocene aridification trend**

389    This study shows that a progressive aridification trend occurred during at least the last ca. 4700
390    cal yr BP in the southern Iberian Peninsula. The increase in aridity is shown in the Padul-15-05
391    core by a progressive decrease in Mediterranean forest component and the increase in herbs
392    (Figs. 4 and 7). Lake level interpretations from our record agree with the pollen and show an
393    overall decrease during the Late Holocene, from a shallow water table containing relatively
394    abundant organic matter (high TOC, indicating higher productivity), gastropods and charophytes
395    (high Ca values) to a low-productive ephemeral/emerged environment (high clastic input and MS
396    and decrease in Ca) (Fig. 5). This progressive aridification confirmed by the increase in
397    siliciclastics pointing to a change towards ephemeral (even emerged) environments became more
398    prominent since the last ca. 1550 cal yr BP and then enhanced again in the last 300 cal yr BP to
399    Present. *Glomus*, a spore from mycorrhizal fungi that occur in soils (van Geel et al., 1989),
400    follows a similar pattern of change, which probably points to enhanced soil erosion in the
401    catchment area during the last 1550 cal yr BP. Furthermore, the increase in some proxies
402    indicating human land use during this last period suggests that humans were more active in this
403    area since then.
404    These results are supported by previous studies from the Mediterranean area using different
405    proxies documenting an aridification trend since the Middle Holocene (Carrión, 2002; Carrión et
406    al., 2010a; Fletcher et al., 2013; Fletcher and Sánchez-Goñi, 2008; Jiménez-Espejo et al., 2014;
407    Jiménez-Moreno et al., 2015). In the western Mediterranean region this decline in forest
408    development during the Middle and Late Holocene is related with a decrease in summer
409    insolation (Fletcher et al., 2013; Jiménez-Moreno and Anderson, 2012). This would produce a
410    progressive cooling, with a reduction in the length of the growing season as well as a decrease in
411    the sea-surface temperature (Marchal et al., 2002), generating a decrease in the land-sea contrast
412    that would be reflected in a reduction of the wind system and a reduced precipitation gradient
413    from sea to shore during the fall-winter season. Also, a reorganization of the general atmospheric
414    circulation with a northward shift of the westerlies - a long-term enhanced positive NAO trend -
415    has been interpreted, inducing drier conditions in this area since 6000 cal yr BP (Magny et al.,
416    2012). The aridification trend can clearly be seen in the nearby alpine records from the Sierra
417    Nevada, where there was little influence by human activity (Anderson et al., 2011; Jiménez-
418    Moreno et al., 2013; Jiménez-Moreno and Anderson, 2012; Ramos-Román et al., 2016).

419    **5.2 Millennial- and centennial-scale climate variability in the Padul peat bog during the**
420    **Late Holocene**

421    The multi-proxy paleoclimate record from Padul-15-05 shows an overall aridification trend.
422    However, this trend seems to be modulated by millennial- and centennial-scale climatic
423    variability.

424    **5.2.1 Aridity pulses around 4200 (4500, 4300 and 4000 cal yr BP) and around 3000 cal yr**
425    **BP (3300 and 2800 cal yr BP)**

426  Marked aridity pulses are registered in the Padul-15-05 record around 4200 and 3000 cal yr BP
427  (Unit 1; Pollen zones 1 an 2a; Figs. 6 and 7). These arid pulses are mostly evidenced in this
428  record by declines in Mediterranean forest taxa, as well as lake level drops and/or cooling
429  evidenced by a decrease in organic component as TOC and the decrease in *Botryococcus* algae.
430  However, a discrepancy between the local and regional occurs between 3000-2800 cal yr BP,
431  with an increase in the estimated lake level and a decrease in the Mediterranean forest during the
432  late Bronze Age until the early Iron Age (Figs. 6 and 7). The disagreement could be due to
433  deforestation by humans during a very active period of mining in the area observed as a peak in
434  lead pollution in the alpine records from Sierra Nevada (García-Alix et al., 2013) . The aridity
435  pulses agree regionally with recent studies carried out at higher in elevation in the Sierra Nevada,
436  a decrease in AP percentage in Borreguil de la Caldera record around 4000-3500 cal yr BP
437  (Ramos-Román et al., 2016), high percentage of non-arboreal pollen around 3400 cal ka BP in
438  Zoñar lake [Southern Córdoba Natural Reserve; (Martín-Puertas et al., 2008)], and lake
439  desiccation at ca. 4100 and 2900 cal yr BP in Lake Siles (Carrión et al., 2007). Jalut et al. (2009)
440  compared paleoclimatic records from different lakes in the western Mediterranean region and
441  also suggested a dry phase between 4300 to 3400 cal yr BP, synchronous with this aridification
442  phase. Furthermore, in the eastern Mediterranean basin other pollen studies show a decrease in
443  arboreal pollen concentration toward more open landscapes around 3.7 ka cal BP (Magri, 1999).
444  Significant climatic changes also occurred in the Northern Hemisphere at those times and polar
445  cooling and tropical aridity are observed at ca. 4200-3800 and 3500-2500 cal yr BP; (Mayewski
446  et al., 2004), cold events in the North Atlantic [cold event 3 and 2; (Bond et al., 2001)], decrease
447  in solar irradiance (Steinhilber et al., 2009) and humidity decreases in the eastern Mediterranean
448  area at 4200 cal yr BP (Bar-Matthews et al., 2003) that could be related with global scale climate
449  variability (Fig. 6). These generally dry phases between 4.5 and 2.8 in Padul-15-05 are generally
450  in agreement with persistent positive NAO conditions during this time (Olsen et al., 2012).
451  The high-resolution Padul-15-05 record shows that climatic crises such as the one occurred at ca.
452  4200 cal yr BP, which seems to be recorded worldwide (Booth et al., 2005), are the product of
453  the sum of more than one single climatic event (i.e., ca. 4500, 4300, 4000 cal yr BP) and thus are
454  affected by climatic variability at centennial-scales.

### 5.2.2 Iberian-Roman Humid Period (~2600 to 1600 cal yr BP)

456  High relative humidity is recorded in the Padul-15-05 record between ca. 2600 and 1600 cal yr
457  BP, synchronous with the well-known Iberian-Roman Humid Period (IRHP; between 2600 and
458  1600 cal yr BP; (Martín-Puertas et al., 2009). This is interpreted in our record due to an increase
459  in the Mediterranean forest species at that time (Unit 1; Pollen Zone 2.b; Figs. 6 and 7). In
460  addition, there is a simultaneous increase in *Botryococcus* algae, which is probably related to
461  higher productivity during warmer conditions. Evidence of a wetter climate around this period
462  has also been shown in other regional records and several alpine records from Sierra Nevada. For
463  example, Jiménez-Moreno et al. (2013) studying a sediment record from the Laguna de la Mula,
464  showed an increase in deciduous *Quercus* in correlation with the maximum in algae between
465  2500 to 1850 cal yr BP, also evidencing the most humid period of the Late Holocene. A
466  geochemical study from the Laguna de Río Seco (also in Sierra Nevada) also evidenced humid
467  conditions around 2200 cal yr BP by the decrease in Saharan dust input and the increase in
468  detritic sedimentation into the lake suggesting higher rainfall (Jiménez-Espejo et al., 2014). In
469  addition, Ramos-Román et al. (2016) showed an increase in AP in the Borreguil de la Caldera
470  record around 2200 cal yr BP, suggesting an increase in humidity at that time.

471 Other records from the Iberian Peninsula also show this pattern to wetter conditions during the
472 IRHP. For example, high lake levels are recorded in Zoñar Lake in southern Spain between 2460
473 to 1600 cal yr BP, only interrupted by a relatively arid pulse between 2140 and 1800 cal yr BP
474 (Martín-Puertas et al., 2009). An increase in rainfall is described in the central region of the
475 Iberian Peninsula in a study from the Tablas de Daimiel National Park between 2100 and 1680
476 cal yr BP (Gil García et al., 2007). Deeper lake levels at around 2650 to 1580 cal yr BP, also
477 interrupted by an short arid event at ca. 2125-1790 cal yr BP, were observed to the north, in the
478 Iberian Range (Currás et al., 2012). The fact that the Padul-15-05 record also shows a relatively
479 arid-cold event between 2150-2050 cal yr BP, just in the middle of this relative humid-warm
480 period, seems to point to a common feature of centennial-scale climatic variability in many
481 western Mediterranean and North Atlantic records (Fig. 6). Humid climate conditions at around
482 2500 cal yr BP are also interpreted in previous studies from lake level reconstructions from
483 Central Europe (Magny, 2004). Increases in temperate deciduous forest are also observed in
484 marine records from the Alboran Sea around 2600 to 2300 cal yr BP, also pointing to high
485 relative humidity (Combourieu Nebout et al., 2009; Fletcher et al., 2007). Overall humid
486 conditions between 2600 and 1600 cal yr BP seem to agree with predominant negative NAO
487 reconstructions at that time, which would translate into greater winter (and thus more effective)
488 precipitation in the area triggering more development of forest species in the area.
489 Generally warm conditions are interpreted between 1900 and 1700 cal yr BP in the
490 Mediterranean Sea, with high sea surface temperatures (SSTs), and in the North Atlantic area,
491 with the decrease in Drift Ice Index. In addition, persistent positive solar irradiance occurred at
492 that time. The increase in *Botryococcus* algae reaching maxima during the IRHP also seems to
493 point to very productive and perhaps warmer conditions in the Padul peat bog area (Fig. 6).

494 **5.2.3 DA and MCA – aridity between ~1550 cal yr BP and 600 cal yr BP**

495 Enhanced aridity occurred right after the IRHP in the Padul peat bog area between ca. 1550 and
496 600 cal yr BP (ca. 400 - 1350 CE). This is deduced in the Padul-15-05 record by a significant
497 forest decline, with a prominent decrease in Mediterranean forest, an increase in Cichorioideae
498 herbs and the decline in the estimated water level (Unit 1; Pollen Zone 3; Figs. 4 and 7). A
499 significant change since the end of the IRHP took place in the lake environment, suggesting the
500 transition from a shallow water table to an ephemeral environment. This is deduced by the
501 disappearance of charophytes, a significant decrease in Algae component and higher Si and MS
502 and lower TOC values (Unit 1; Figs. 6 and 7).
503 This arid phase could be separated into two different periods. The first period occurred between
504 ca. 1550 cal yr BP (ca. 400 CE) and ca. 1100 cal yr BP (ca. 900 CE) and is characterized by a
505 decreasing trend in Mediterranean forest and *Botryococcus* taxa and the increase in
506 Cichorioideae. This period corresponds with the Dark Ages [from ca. 500 to 900 CE; (Moreno et
507 al., 2012)]. A visual correlation between the decrease in Mediterranean forest, the increase in the
508 Drift Ice Index in the North Atlantic record (cold event 1; Bond et al., 2001), the decrease in
509 SSTs in the Mediterranean Sea and maxima in positive NAO reconstructions suggests drier and
510 colder conditions during this time (Fig. 6). Other Mediterranean and central-European records
511 agree with our climate interpretations, for example, a decrease in forest extent is shown in a
512 marine record from the Alboran Sea (Fletcher et al., 2013) and a decrease in lake levels is also
513 observed in Central Europe (Magny et a., 2004) pointing to aridity during the DA. Evidences of
514 aridity during the DA have been show too in the Mediterranean part of the Iberian Peninsula, for
515 instance, cold and arid conditions were suggested in the northern Betic Range by the increase in

516     xerophytic herbs around 1450 and 750 cal yr BP (Carrión et al., 2001a) and in southeastern Spain
517     by a forest decline in lacustrine deposits around 1620 and 1160 cal yr BP (Carrión et al., 2003).
518     Arid and colder conditions during the Dark Ages (around 1680 to 1000 cal yr BP) are also
519     suggested for the central part of the Iberian Peninsula using a multiproxy study of a sediment
520     record from the Tablas de Daimiel Lake (Gil García et al., 2007).
521     A second period that we could differentiate within this overall arid phase occurred around 1100
522     to 600 cal yr BP/900 to 1350 CE, during the well-known MCA (900 to 1300 CE after Moreno et
523     al., 2012). During this period the Padul-15-05 record shows a slight increasing trend in the
524     Mediterranean forest taxa with respect to the DA, but the decrease in *Botryococcus* and the
525     higher abundance of herbs still point to overall arid conditions. This change could be related to
526     an increase in temperature, favoring the development of temperate forest species, and would
527     agree with inferred increasing temperatures in the North Atlantic areas, as well as the increase in
528     solar irradiance and the increase in SSTs in the Mediterranean Sea (Fig.7). This hypothesis
529     would agree with the reconstruction of persistent positive NAO and overall warm conditions
530     during the MCA in the western Mediterranean (see synthesis in Moreno et al., 2012). A similar
531     pattern of increasing xerophytic vegetation during the MCA is observed in alpine peat bogs and
532     lakes in the Sierra Nevada (Anderson et al., 2011; Jiménez-Moreno et al., 2013; Ramos-Román
533     et al., 2016) and arid conditions are shown to occur during the MCA in southern and eastern
534     Iberian Peninsula deduced by increases in salinity and lower lake levels (Corella et al., 2013;
535     Martín-Puertas et al., 2011). However, humid conditions have been reconstructed for the
536     northwestern of the Iberian Peninsula at this time (Lebreiro et al., 2006; Moreno et al., 2012), as
537     well as northern Europe (Martín-Puertas et al., 2008). The different pattern of precipitation
538     between the northwestern Iberian Peninsula / northern Europe and the Mediterranean area is
539     undoubtedly a function of the well-known NAO dipole in precipitation pattern (Trouet et al.,
540     2009).

### 541     5.2.4 The last ~600 cal yr BP: LIA (1350-1850 CE) and IE (1850 CE-Present)

542     Two climatically different periods can be distinguished during the last ca. 600 cal yr BP (end of
543     Zone 3b to Zone 4; Fig. 4) in the area. However, the climatic signal is more difficult to interpret
544     due to a higher human impact at that time. The first phase around 1350-1450 CE was
545     characterized by increasing relative humidity by the decrease in xerophytes and the increase in
546     Mediterranean forest taxa and *Botryococcus* after a period of decrease during the DA and MCA,
547     corresponding to the LIA. The second phase is characterized here by the decrease in the
548     Mediterranean forest around 1700-1850 CE, pointing to a return to more arid conditions during
549     the last part of the LIA (Figs. 4 and 7). This climatic pattern agrees with an increase in
550     precipitation by the transition from positive to negative NAO mode and from warmer to cooler
551     conditions in the North Atlantic area during the first phase of the LIA and a second phase
552     characterized by cooler (cold event 0; Bond et al., 2001) and drier conditions (Fig. 6). A stronger
553     variability in the SSTs is described in the Mediterranean Sea during the LIA (Fig. 6). Mayewski
554     et al. (2004) described a period of climate variability during the Holocene at this time (600 to
555     150 cal yr BP) suggesting a polar cooling but more humid in some parts of the tropics.
556     Regionally, (Morellón et al., 2011) also described a phase of more humid conditions between
557     1530 to 1750 CE in a lake sediment record from NE Spain. An alternation between wetter to
558     drier periods during the LIA are also shown in the nearby alpine record from Borreguil de la
559     Caldera in the Sierra Nevada mountain range (Ramos-Román et al., 2016).

560   The environmental transition from ephemeral to emerged conditions, observed in the last ca.
561   1550 cal yr BP (Unit 1; Fig. 5), intensified in the last ca. 300 cal yr BP. This is shown by the
562   highest MS and Si values the increase in wetland plants and the stronger decrease in Ca and
563   organic components (TOC) in the sediments in the uppermost part of the Padul-15-05 record
564   (Unit 2; Figs. 3 and 6).

565   **5.3 Centennial-scale variability**

566   Time series analysis has become important in determining the recurrent periodicity of cyclical
567   oscillations in paleoenvironmental sequences (e.g. Jiménez-Espejo et al., 2014; Ramos-Román et
568   al., 2016; Rodrigo-Gámiz et al., 2014; Fletcher et al., 2013). This analysis also assists in
569   understanding possible relationships between the paleoenvironmental proxy data and the
570   potential triggers of the observed cyclical changes: i.e., solar activity, atmospheric, oceanic
571   dynamics and climate evolution during the Holocene. The cyclostratigraphic analysis on the
572   pollen (Mediterranean forest; regional signal), algae (*Botryococcus*; local signal) and TOC (local
573   signal) times series from the Padul-15-05 record evidence centennial-scale cyclical patterns with
574   periodicities around 800, 680, 300, 240, 200 and 170 years above the 90 % confidence levels
575   (Fig. 7).
576   Previous cyclostratigraphic analysis in Holocene western Mediterranean records suggest cyclical
577   climatic oscillations with periodicities around 1500 and 1750 yr (Fletcher et al., 2013; Jiménez-
578   Espejo et al., 2014; Rodrigo-Gámiz et al., 2014). Other North Atlantic and Mediterranean
579   records also present cyclicities in their paleoclimatic proxies of ca. 1600 yr (Bond et al., 2001;
580   Debret et al., 2007; Rodrigo-Gámiz et al., 2014). However, this cycle is absent from the
581   cyclostratigraphic analysis in the Padul-15-05 record (Fig. 7). In contrast, the spectral analysis
582   performed in the Mediterranean forest time series from Padul peat bog record, pointing to
583   cyclical hydrological changes, shows a significant ~800 yr cycle that could be related to solar
584   variability (Damon and Sonett, 1991) or could be the second harmonic of the ca. ~1600 yr
585   oceanic-related cycle (Debret et al., 2009). A very similar periodicity of ca. 760 yr is detected in
586   the *Pinus* forest taxa, also pointing to humidity variability, from the alpine Sierra Nevada site of
587   Borreguil de la Caldera and seems to show that this is a common feature of cyclical
588   paleoclimatic oscillation in the area.
589   A significant ~680 cycle is shown in the *Botryococcus* time series most likely suggesting
590   recurrent centennial-scale changes in temperature (productivity) and water availability. A similar
591   cycle is shown in the *Artemisia* signal in an alpine record from Sierra Nevada (Ramos-Román et
592   al., 2016). This cycle around ~650 yr is also observed in a marine record from the Alboran Sea,
593   and was interpreted as the secondary harmonic of the 1300 yr cycle that those authors related
594   with cyclic thermohaline circulation and sea surface temperature changes (Rodrigo-Gámiz et al.,
595   2014).
596   A statistically significant ~300 yr cycle is shown in the Mediterranean forest taxa and TOC from
597   the Padul-15-05 record suggesting shorter-scale variability in water availability. This cycle is
598   also observed in the cyclical *Pinus* pollen data from Borreguil de la Caldera at higher elevations
599   in the Sierra Nevada (Ramos-Román et al., 2016). This cycle could be principally related to
600   NAO variability as observed by Olsen et al. (2012), which follows variations in humidity
601   observed in the Padul-15-05 record. NAO variability also regulates modern precipitation in the
602   area.
603   The *Botryococcus* and TOC time series shows variability with a periodicity around ~240, 200
604   and 164 yrs. Sonnet et al. (1984) described a significant cycle in solar activity around ~208 yr

605 (Suess solar cycle), which could have triggered our ~200 cyclicity. The observed ~240 yr
606 periodicity in the Padul-15-05 record could be either related to variations in solar activity or due
607 to the mixed effect of the solar together with the ~300 yr NAO-interpreted cycle and could point
608 to a solar origin of the centennial-scale NAO variations as suggested by previously published
609 research (Lukianova and Alekseev, 2004; Zanchettin et al., 2008). Finally, a significant ~170 yr
610 cycle has been observed in both the Mediterranean forest taxa and *Botryococcus* times series
611 from the Padul-15-05 record. A similar cycle (between 168-174 yr) was also described in the
612 alpine pollen record from Borreguil de la Caldera in Sierra Nevada (Ramos-Román et al., 2016),
613 which shows that it is a significant cyclical pattern in climate, probably precipitation, in the area.
614 This cycle could be related to the previously described ~170 yr cycle in the NAO index (Olsen et
615 al., 2012), which would agree with the hypothesis of the NAO controlling millennial- and
616 centennial-scale environmental variability during the Late Holocene in the area (García-Alix et
617 al., 2017; Ramos-Román et al., 2016).

618 **5.4 Human activity**

619 Humans probably had an impact in the area since Prehistoric times, however, the Padul-15-05
620 multiproxy record shows a more significant human impact during the last ca. 1550 cal yr BP,
621 which intensified in the last ca. 500 cal yr BP (since 1450 CE to Present). This is deduced by, a
622 significant increase in nitrophilous plant taxa such as Cichorioideae, Convolvulaceae,
623 Polygonaceae and *Plantago* and the increase in some NPP such as *Tilletia*, coprophilous fungi
624 and thecamoebians (Unit 2; Pollen Zone 4; Fig. 4). Most of these pollen taxa and NPPs are
625 described in other southern Iberian paleoenvironmental records as indicators of land uses, for
626 instance, *Tilletia* and covarying Cichorioideae and Convolvulaceae have been described as
627 indicators of farming (e.g. Carrión et al., 2001b). Interestingly, these taxa being to decline around
628 ~1450 CE, coinciding with the higher increase in detritic material into the basin. Climatically,
629 this event coincides with the start of persistent negative NAO conditions in the area (Trouet et
630 al., 2009), which could have further triggered more rainfall and more detritic input into the basin.
631 Bellin et al., 2011 in a study from the Betic Cordillera (southern Iberian Peninsula) demonstrate
632 that soil erosion increase in years with higher rainfall and this could be intensified by human
633 impact. Nevertheless, in a study in the southeastern part of the Iberian Peninsula (Bellin et al.,
634 2013) suggested that major soil erosion could have occurred by the abandonment of agricultural
635 activities in the mountain areas as well as the abandonment of irrigated terrace systems during
636 the Christian Reconquest. Enhanced soil erosion at this time is also supported by the increase in
637 *Glomus* type (Fig. 4).
638 An important change in the sedimentation in the environment is observed during the last ca. 300
639 cal yr BP marked by the stronger increase in MS and Si values. This was probably related with
640 the Padul peat bog water drainage by humans using canals in the late XVIII century for
641 cultivation purposes (Villegas Molina, 1967). The increase in wetland vegetation and higher
642 values of Poaceae could be due to cultivation of cereals or by an increase in the population of
643 *Phragmites australis* (also a Poaceae), very abundant in the Padul peat bog margins at present
644 due to the increase in drained land surface.
645 The uppermost part (last ca. 100 cal yr BP) of the pollen record from Padul-15-05 shows an
646 increasing trend in some arboreal taxa at that time, including Mediterranean forest, *Olea* and
647 *Pinus* (Fig. 4). This change is most likely of human origin and generated by the increase in *Olea*
648 cultivation in the last two centuries, also observed in many records from higher elevation sites
649 from Sierra Nevada, and *Pinus* and other Mediterranean species reforestation in the 20th century

650    (Anderson et al., 2011; Jiménez-Moreno and Anderson, 2012; Jiménez-Moreno et al., 2013;
651    Ramos-Román et al., 2016).

652    **6 Conclusions**

653    Our multiproxy (i.e. lithology, geochemistry, paleontology) analysis from the Padul-15-05
654    sequence has provided a detailed climate reconstruction for the last 4700 ca yr BP for the Padul
655    peat bog area and the western Mediterranean. This study, supported by the comparison with
656    other Mediterranean and North Atlantic records suggests a link between vegetation, atmospheric
657    dynamics and insolation and solar activity during the Late Holocene in this area. A climatic
658    aridification trend occurred during the Late Holocene in the Sierra Nevada and the western
659    Mediterranean area, probably linked with the orbital-scale decreasing trend in summer
660    insolation. This long-term trend is modulated by centennial-scale climate variability as shown by
661    the pollen (Mediterranean forest taxa) algae (*Botryococcus*) and sedimentary and geochemical
662    data in the Padul record. These events are in correlation with regional and global scale climate
663    variability and cold and arid pulses around the 4200 and 3000 cal yr BP that are identified in this
664    study seem to be synchronous with cold events recorded in the North Atlantic and decreases in
665    precipitation in the Mediterranean area, probably linked to persistent positive NAO mode.
666    Moreover, one of the most important humid and warmer periods during the Late Holocene in the
667    Padul area coincides in time with the well-known IRHP, warm and humid conditions in the
668    Mediterranean and North Atlantic regions and overall negative NAO conditions. A drastic
669    decrease in Mediterranean forest taxa towards an open landscape, pointing to colder and
670    enhanced aridity, occurred in two steps (DA and end of the LIA) during the last ca. 1550 cal yr
671    BP. However, this trend was slightly superimposed by a more arid but warmer event coinciding
672    with the MCA and a cold but wetter event during the first part of the LIA. Besides natural
673    climatic and environmental variability, there seems to be intense human activities in the area
674    during the last the last ca. 1550 cal yr BP. This suggests that the natural aridification trend during
675    the Late Holocene in the western Mediterranean region could have been intensified due to the
676    higher human activity in this area.
677    Furthermore, time series analyses done in the Padul-15-05 record show centennial-scale changes
678    in the environment and climate that are coincident with the periodicities observed in solar,
679    oceanic and NAO reconstructions and could show a close cause-and-effect linkage between
680    them.

681    **Acknowledgement**

682    This work was supported by the project P11-RNM-7332 funded by Consejería de Economía,
683    Innovación, Ciencia y Empleo de la Junta de Andalucía, the project CGL2013-47038-R funded
684    by Ministerio de Economía y Competitividad of Spain and fondo Europeo de desarrollo regional
685    FEDER and the research group RNM0190 (Junta de Andalucía). M. J. R.-R. acknowledges the
686    PhD funding provided by Consejería de Economía, Innovación, Ciencia y Empleo de la Junta de
687    Andalucía (P11-RNM-7332). J.C. acknowledges the PhD funding provided by Ministerio de
688    Economía y Competitividad (CGL2013-47038-R). A.G.-A. was also supported by a Ramón y
689    Cajal Fellowship RYC-2015-18966 of the Spanish Government (Ministerio de Economía y
690    Competitividad). Javier Jaimez (CIC-UGR) is thanked for graciously helping with the coring, the
691    drilling equipment and logistics.

# References

Abel-Schaad, D. and López-Sáez, J. A.: Vegetation changes in relation to fire history and human activities at the Peña Negra mire (Bejar Range, Iberian Central Mountain System, Spain) during the past 4,000 years, Veg. Hist. Archaeobotany, 22(3), 199–214, doi:10.1007/s00334-012-0368-9, 2013.

Al Aallali, A., Nieto, J. M. L., Raya, F. A. P. and Mesa, J. M.: Estudio de la vegetación forestal en la vertiente sur de Sierra Nevada (Alpujarra Alta granadina), Itinera Geobot., (11), 387–402, 1998.

Alfaro, P., Galinod-Zaldievar, J., Jabaloy, A., López-Garrido, A. C. and Sanz de Galdeano, C.: Evidence for the activity and paleoseismicity of the Padul fault (Betic Cordillera, Southern Spain) [Evidencias de actividad y paleosismicidad de la falla de Padul (Cordillera Bética, sur de España)], Acta Geol. Hisp., 36(3–4), 283–297, 2001.

Alpert, P., Baldi, M., Ilani, R., Krichak, S., Price, C., Rodó, X., Saaroni, H., Ziv, B., Kishcha, P., Barkan, J., Mariotti, A. and Xoplaki, E.: Chapter 2 Relations between climate variability in the Mediterranean region and the tropics: ENSO, South Asian and African monsoons, hurricanes and Saharan dust, Dev. Earth Environ. Sci., 4(C), 149–177, doi:10.1016/S1571-9197(06)80005-4, 2006.

Anderson, R. S., Jiménez-Moreno, G., Carrión, J. S. and Pérez-Martínez, C.: Postglacial history of alpine vegetation, fire, and climate from Laguna de Río Seco, Sierra Nevada, southern Spain, Quat. Sci. Rev., 30(13–14), 1615–1629, doi:https://doi.org/10.1016/j.quascirev.2011.03.005, 2011.

Bar-Matthews, M., Ayalon, A., Gilmour, M., Matthews, A. and Hawkesworth, C. J.: Sea–land oxygen isotopic relationships from planktonic foraminifera and speleothems in the Eastern Mediterranean region and their implication for paleorainfall during interglacial intervals, Geochim. Cosmochim. Acta, 67(17), 3181–3199, doi:https://doi.org/10.1016/S0016-7037(02)01031-1, 2003.

Bellin, N., Vanacker, V., van Wesemael, B., Solé-Benet, A. and Bakker, M. M.: Natural and anthropogenic controls on soil erosion in the internal betic Cordillera (southeast Spain), Catena, 87(2), 190–200, doi:10.1016/j.catena.2011.05.022, 2011.

Bellin, N., Vanacker, V. and De Baets, S.: Anthropogenic and climatic impact on Holocene sediment dynamics in SE Spain: A review, Quat. Int., 308–309, 112–129, doi:10.1016/j.quaint.2013.03.015, 2013.

Beug, H.-J.: Leitfaden der Pollenbestimmung für Mitteleuropa und angrenzende Gebiete, Fisch. Stuttg., 61, 1961.

Blaauw, M.: Methods and code for "classical" age-modelling of radiocarbon sequences, Quat. Geochronol., 5(5), 512–518, doi:https://doi.org/10.1016/j.quageo.2010.01.002, 2010.

727   Bond, G., Kromer, B., Beer, J., Muscheler, R., Evans, M. N., Showers, W., Hoffmann, S., Lotti-
728   Bond, R., Hajdas, I. and Bonani, G.: Persistent Solar Influence on North Atlantic Climate During
729   the Holocene, Science, 294(5549), 2130, doi:10.1126/science.1065680, 2001.

730   Booth, R. K., Jackson, S. T., Forman, S. L., Kutzbach, J. E., E. A. Bettis, I., Kreigs, J. and Wright, D.
731   K.: A severe centennial-scale drought in midcontinental North America 4200 years ago and
732   apparent global linkages, The Holocene, 15(3), 321–328, doi:10.1191/0959683605hl825ft,
733   2005.

734   Carrión, J. S.: Patterns and processes of Late Quaternary environmental change in a montane
735   region of southwestern Europe, Quat. Sci. Rev., 21(18–19), 2047–2066,
736   doi:https://doi.org/10.1016/S0277-3791(02)00010-0, 2002.

737   Carrión, J. S., Munuera, M., Dupré, M. and Andrade, A.: Abrupt vegetation changes in the
738   Segura Mountains of southern Spain throughout the Holocene, J. Ecol., 89(5), 783–797,
739   doi:10.1046/j.0022-0477.2001.00601.x, 2001a.

740   Carrión, J. S., Andrade, A., Bennett, K. D., Navarro, C. and Munuera, M.: Crossing forest
741   thresholds: inertia and collapse in a Holocene sequence from south-central Spain, The
742   Holocene, 11(6), 635–653, doi:10.1191/09596830195672, 2001b.

743   Carrión, J. S., Fernández, S., Jiménez-Moreno, G., Fauquette, S., Gil-Romera, G., González-
744   Sampériz, P. and Finlayson, C.: The historical origins of aridity and vegetation degradation in
745   southeastern Spain, J. Arid Environ., 74(7), 731–736,
746   doi:https://doi.org/10.1016/j.jaridenv.2008.11.014, 2010b.

747   Carrión, J. S., Sánchez-Gómez, P., Mota, J. F., Yll, R. and Chaín, C.: Holocene vegetation
748   dynamics, fire and grazing in the Sierra de Gádor, southern Spain, Holocene, 13(6), 839–849,
749   doi:10.1191/0959683603hl662rp, 2003.

750   Carrión, J. S., Fuentes, N., González-Sampériz, P., Quirante, L. S., Finlayson, J. C., Fernández, S.
751   and Andrade, A.: Holocene environmental change in a montane region of southern Europe with
752   a long history of human settlement, Quat. Sci. Rev., 26(11–12), 1455–1475,
753   doi:https://doi.org/10.1016/j.quascirev.2007.03.013, 2007.

754   Carrión, J. S., Fernández, S., González-Sampériz, P., Gil-Romera, G., Badal, E., Carrión-Marco, Y.,
755   López-Merino, L., López-Sáez, J. A., Fierro, E. and Burjachs, F.: Expected trends and surprises in
756   the Lateglacial and Holocene vegetation history of the Iberian Peninsula and Balearic Islands,
757   Rev. Palaeobot. Palynol., 162(3), 458–475,
758   doi:http://dx.doi.org/10.1016/j.revpalbo.2009.12.007, 2010.

759   Combourieu-Nebout, N., Peyron, O., Dormoy, I., Desprat, S., Beaudouin, C., Kotthoff, U. and
760   Marret, F.: Rapid climatic variability in the west Mediterranean during the last 25 000 years
761   from high resolution pollen data, Clim Past, 5(3), 503–521, doi:10.5194/cp-5-503-2009, 2009.

762   Corella, J. P., Stefanova, V., El Anjoumi, A., Rico, E., Giralt, S., Moreno, A., Plata-Montero, A. and

763   Valero-Garcés, B. L.: A 2500-year multi-proxy reconstruction of climate change and human
764   activities in northern Spain: The Lake Arreo record, Palaeogeogr. Palaeoclimatol. Palaeoecol.,
765   386, 555–568, doi:10.1016/j.palaeo.2013.06.022, 2013.

766   Currás, A., Zamora, L., Reed, J. M., García-Soto, E., Ferrero, S., Armengol, X., Mezquita-Joanes,
767   F., Marqués, M. A., Riera, S. and Julià, R.: Climate change and human impact in central Spain
768   during Roman times: High-resolution multi-proxy analysis of a tufa lake record (Somolinos,
769   1280m asl), Catena, 89(1), 31–53, doi:10.1016/j.catena.2011.09.009, 2012.

770   Damon, P. E. and Sonett, C. P.: Solar and terrestrial components of the atmospheric C-14
771   variation spectrum. In: Sonett, C.P., Giampapa, M.S., Matthews, M.S. (Eds.), The Sun in Time.
772   University of Arizona Press, Tucson, AZ, USA., 1991.

773   Debret, M., Bout-Roumazeilles, V., Grousset, F., Desmet, M., McManus, J. F., Massei, N., Sebag,
774   D., Petit, J.-R., Copard, Y. and Trentesaux, A.: The origin of the 1500-year climate cycles in
775   holocene north-atlantic records, Clim. Past, 3(4), 569–575, 2007.

776   Debret, M., Sebag, D., Crosta, X., Massei, N., Petit, J.-R., Chapron, E. and Bout-Roumazeilles, V.:
777   Evidence from wavelet analysis for a mid-Holocene transition in global climate forcing, Quat.
778   Sci. Rev., 28(25–26), 2675–2688, doi:https://doi.org/10.1016/j.quascirev.2009.06.005, 2009.

779   Delgado, J., Alfaro, P., Galindo-Zaldivar, J., Jabaloy, A., Lopez Garrido, A. and Sanz de Galdeano,
780   C.: Structure of the Padul-Nigüelas basin (S Spain) from H/V ratios of ambient noise: application
781   of the method to study peat and coarse sediments, Pure Appl. Geophys., 159(11), 2733–2749,
782   2002.

783   Domingo-García, M., Fernández-Rubio, R., Lopez, J. and González, C.: Aportación al
784   conocimiento de la Neotectónica de la Depresión del Padul (Granada), Tecniterrae, 53, 6–16,
785   1983.

786   Ejarque, A., Anderson, R. S., Simms, A. R. and Gentry, B. J.: Prehistoric fires and the shaping of
787   colonial transported landscapes in southern California: A paleoenvironmental study at Dune
788   Pond, Santa Barbara County, Quat. Sci. Rev., 112, 181–196,
789   doi:https://doi.org/10.1016/j.quascirev.2015.01.017, 2015.

790   Faegri, K. and Iversen, J.: Textbook of Pollen Analysis. Wiley, New York., 1989.

791   Fletcher, W. J. and Sánchez-Goñi, M. F.: Orbital- and sub-orbital-scale climate impacts on
792   vegetation of the western Mediterranean basin over the last 48,000 yr, Quat. Res., 70(3), 451–
793   464, doi:10.1016/j.yqres.2008.07.002, 2008.

794   Fletcher, W. J., Debret, M. and Sánchez-Goñi, M. F.: Mid-Holocene emergence of a low-
795   frequency millennial oscillation in western Mediterranean climate: Implications for past
796   dynamics of the North Atlantic atmospheric westerlies, The Holocene, 23(2), 153–166,
797   doi:10.1177/0959683612460783, 2013.

798   Florschütz, F., Amor, J. M. and Wijmstra, T. A.: Palynology of a thick quaternary succession in
799   southern Spain, Palaeogeogr. Palaeoclimatol. Palaeoecol., 10(4), 233–264,
800   doi:http://dx.doi.org/10.1016/0031-0182(71)90049-6, 1971.

801   García-Alix, A., Jimenez-Espejo, F. J., Lozano, J. A., Jiménez-Moreno, G., Martinez-Ruiz, F.,
802   Sanjuán, L. G., Jiménez, G. A., Alfonso, E. G., Ruiz-Puertas, G. and Anderson, R. S.:
803   Anthropogenic impact and lead pollution throughout the Holocene in Southern Iberia, Sci. Total
804   Environ., 449, 451–460, doi:https://doi.org/10.1016/j.scitotenv.2013.01.081, 2013.

805   García-Alix, A., Jiménez-Espejo, F. J., Toney, J. L., Jiménez-Moreno, G., Ramos-Román, M. J.,
806   Anderson, R. S., Ruano, P., Queralt, I., Delgado Huertas, A. and Kuroda, J.: Alpine bogs of
807   southern Spain show human-induced environmental change superimposed on long-term
808   natural variations, Sci. Rep., 7(1), 7439, doi:10.1038/s41598-017-07854-w, 2017.

809   van Geel, B., Hallewas, D. P. and Pals, J. P.: A late holocene deposit under the Westfriese Zeedijk
810   near Enkhuizen (Prov. of Noord-Holland, The Netherlands): Palaeoecological and archaeological
811   aspects, Rev. Palaeobot. Palynol., 38(3), 269–335, doi:http://dx.doi.org/10.1016/0034-
812   6667(83)90026-X, 1983.

813   van Geel, B., Coope, G. R. and Hammen, T. V. D.: Palaeoecology and stratigraphy of the
814   lateglacial type section at Usselo (the Netherlands), Rev. Palaeobot. Palynol., 60(1), 25–129,
815   doi:http://dx.doi.org/10.1016/0034-6667(89)90072-9, 1989.

816   Gil García, M. J., Ruiz Zapata, M. B., Santisteban, J. I., Mediavilla, R., López-Pamo, E. and Dabrio,
817   C. J.: Late holocene environments in Las Tablas de Daimiel (south central Iberian peninsula,
818   Spain), Veg. Hist. Archaeobotany, 16(4), 241–250, doi:10.1007/s00334-006-0047-9, 2007.

819   Gil-Romera, G., González-Sampériz, P., Lasheras-Álvarez, L., Sevilla-Callejo, M., Moreno, A.,
820   Valero-Garcés, B., López-Merino, L., Carrión, J. S., Pérez Sanz, A., Aranbarri, J. and García-Prieto
821   Fronce, E.: Biomass-modulated fire dynamics during the Last Glacial–Interglacial Transition at
822   the Central Pyrenees (Spain), Palaeogeogr. Palaeoclimatol. Palaeoecol., 402, 113–124,
823   doi:https://doi.org/10.1016/j.palaeo.2014.03.015, 2014.

824   Grimm, E. C.: CONISS: a FORTRAN 77 program for stratigraphically constrained cluster analysis
825   by the method of incremental sum of squares, Comput. Geosci., 13(1), 13–35,
826   doi:http://dx.doi.org/10.1016/0098-3004(87)90022-7, 1987.

827   Guy-Ohlson, D.: Botryococcus as an aid in the interpretation of palaeoenvironment and
828   depositional processes, Rev. Palaeobot. Palynol., 71(1), 1–15,
829   doi:http://dx.doi.org/10.1016/0034-6667(92)90155-A, 1992.

830   Hurrell, J. W.: Decadal Trends in the North Atlantic Oscillation: Regional Temperatures and
831   Precipitation, Science, 269(5224), 676, doi:10.1126/science.269.5224.676, 1995.

832   Jalut, G., Dedoubat, J. J., Fontugne, M. and Otto, T.: Holocene circum-Mediterranean vegetation
833   changes: Climate forcing and human impact, Quat. Int., 200(1–2), 4–18,

834    doi:https://doi.org/10.1016/j.quaint.2008.03.012, 2009.

835    Jiménez-Espejo, F. J., García-Alix, A., Jiménez-Moreno, G., Rodrigo-Gámiz, M., Anderson, R. S.,
836    Rodríguez-Tovar, F. J., Martínez-Ruiz, F., Giralt, S., Delgado Huertas, A. and Pardo-Igúzquiza, E.:
837    Saharan aeolian input and effective humidity variations over western Europe during the
838    Holocene from a high altitude record, Chem. Geol., 374–375, 1–12,
839    doi:10.1016/j.chemgeo.2014.03.001, 2014.

840    Jiménez-Moreno, G. and Anderson, R. S.: Holocene vegetation and climate change recorded in
841    alpine bog sediments from the Borreguiles de la Virgen, Sierra Nevada, southern Spain, Quat.
842    Res., 77(1), 44–53, doi:10.1016/j.yqres.2011.09.006, 2012.

843    Jiménez-Moreno, G., García-Alix, A., Hernández-Corbalán, M. D., Anderson, R. S. and Delgado-
844    Huertas, A.: Vegetation, fire, climate and human disturbance history in the southwestern
845    Mediterranean area during the late Holocene, Quat. Res., 79(2), 110–122,
846    doi:https://doi.org/10.1016/j.yqres.2012.11.008, 2013.

847    Jiménez-Moreno, G., Rodríguez-Ramírez, A., Pérez-Asensio, J. N., Carrión, J. S., López-Sáez, J. A.,
848    Villarías-Robles, J. J. R., Celestino-Pérez, S., Cerrillo-Cuenca, E., León, Á. and Contreras, C.:
849    Impact of late-Holocene aridification trend, climate variability and geodynamic control on the
850    environment from a coastal area in SW Spain, Holocene, 25(4), 607–617,
851    doi:10.1177/0959683614565955, 2015.

852    Kalugin, I., Daryin, A., Smolyaninova, L., Andreev, A., Diekmann, B. and Khlystov, O.: 800-yr-long
853    records of annual air temperature and precipitation over southern Siberia inferred from
854    Teletskoye Lake sediments, Quat. Res., 67(3), 400–410,
855    doi:https://doi.org/10.1016/j.yqres.2007.01.007, 2007.

856    Laskar, J., Robutel, P., Joutel, F., Gastineau, M., Correia, A. C. M. and Levrard, B.: A long-term
857    numerical solution for the insolation  quantities of the Earth, A&A, 428(1), 261–285,
858    doi:10.1051/0004-6361:20041335, 2004.

859    Lebreiro, S. M., Francés, G., Abrantes, F. F. G., Diz, P., Bartels-Jónsdóttir, H. B., Stroynowski, Z.
860    N., Gil, I. M., Pena, L. D., Rodrigues, T., Jones, P. D., Nombela, M. A., Alejo, I., Briffa, K. R., Harris,
861    I. and Grimalt, J. O.: Climate change and coastal hydrographic response along the Atlantic
862    Iberian margin (Tagus Prodelta and Muros Ría) during the last two millennia, Holocene, 16(7),
863    1003–1015, doi:10.1177/0959683606hl990rp, 2006.

864    Lillios, K. T., Blanco-González, A., Drake, B. L. and López-Sáez, J. A.: Mid-late Holocene climate,
865    demography, and cultural dynamics in Iberia: A multi-proxy approach, Quat. Sci. Rev., 135, 138–
866    153, doi:https://doi.org/10.1016/j.quascirev.2016.01.011, 2016.

867    López-Sáez, J. A., Abel-Schaad, D., Pérez-Díaz, S., Blanco-González, A., Alba-Sánchez, F., Dorado,
868    M., Ruiz-Zapata, B., Gil-García, M. J., Gómez-González, C. and Franco-Múgica, F.: Vegetation
869    history, climate and human impact in the Spanish Central System over the last 9000 years,

870    Quat. Int., 353, 98–122, doi:https://doi.org/10.1016/j.quaint.2013.06.034, 2014.

871    Lukianova, R. and Alekseev, G.: Long-Term Correlation Between the Nao and Solar Activity, Sol.
872    Phys., 224(1), 445–454, doi:10.1007/s11207-005-4974-x, 2004.

873    Magny, M.: Holocene climate variability as reflected by mid-European lake-level fluctuations
874    and its probable impact on prehistoric human settlements, Quat. Int., 113(1), 65–79,
875    doi:https://doi.org/10.1016/S1040-6182(03)00080-6, 2004.

876    Magny, M., Peyron, O., Sadori, L., Ortu, E., Zanchetta, G., Vannière, B. and Tinner, W.:
877    Contrasting patterns of precipitation seasonality during the Holocene in the south- and north-
878    central Mediterranean, J. Quat. Sci., 27(3), 290–296, doi:10.1002/jqs.1543, 2012.

879    Magri, D.: Late Quaternary vegetation history at Lagaccione near Lago di Bolsena (central Italy),
880    Rev. Palaeobot. Palynol., 106(3–4), 171–208, doi:https://doi.org/10.1016/S0034-
881    6667(99)00006-8, 1999.

882    Marchal, O., Cacho, I., Stocker, T. F., Grimalt, J. O., Calvo, E., Martrat, B., Shackleton, N.,
883    Vautravers, M., Cortijo, E., Van Kreveld, S., Andersson, C., Koç, N., Chapman, M., Sbaffi, L.,
884    Duplessy, J.-C., Sarnthein, M., Turon, J.-L., Duprat, J. and Jansen, E.: Apparent long-term cooling
885    of the sea surface in the northeast Atlantic and Mediterranean during the Holocene, Quat. Sci.
886    Rev., 21(4–6), 455–483, doi:10.1016/S0277-3791(01)00105-6, 2002.

887    Martín-Puertas, C., Valero-Garcés, B. L., Mata, M. P., González-Sampériz, P., Bao, R., Moreno, A.
888    and Stefanova, V.: Arid and humid phases in southern Spain during the last 4000 years: the
889    Zoñar Lake record, Córdoba, The Holocene, 18(6), 907–921, doi:10.1177/0959683608093533,
890    2008.

891    Martín-Puertas, C., Valero-Garcés, B. L., Brauer, A., Mata, M. P., Delgado-Huertas, A. and Dulski,
892    P.: The Iberian-Roman Humid Period (2600-1600 cal yr BP) in the Zoñar Lake varve record
893    (Andalucía, southern Spain), Quat. Res., 71(2), 108–120, doi:10.1016/j.yqres.2008.10.004, 2009.

894    Martín-Puertas, C., Valero-Garcés, B. L., Mata, M. P., Moreno, A., Giralt, S., Martínez-Ruiz, F.
895    and Jiménez-Espejo, F.: Geochemical processes in a Mediterranean Lake: A high-resolution
896    study of the last 4,000 years in Zoñar Lake, southern Spain, J. Paleolimnol., 46(3), 405–421,
897    doi:10.1007/s10933-009-9373-0, 2011.

898    Mayewski, P. A., Rohling, E. E., Stager, J. C., Karlén, W., Maasch, K. A., Meeker, L. D., Meyerson,
899    E. A., Gasse, F., Kreveld, S. van, Holmgren, K., Lee-Thorp, J., Rosqvist, G., Rack, F., Staubwasser,
900    M., Schneider, R. R. and Steig, E. J.: Holocene climate variability, Quat. Res., 62(3), 243–255,
901    doi:https://doi.org/10.1016/j.yqres.2004.07.001, 2004.

902    Morellón, M., Valero-Garcés, B., Vegas-Vilarrúbia, T., González-Sampériz, P., Romero, Ó.,
903    Delgado-Huertas, A., Mata, P., Moreno, A., Rico, M. and Corella, J. P.: Lateglacial and Holocene
904    palaeohydrology in the western Mediterranean region: The Lake Estanya record (NE Spain),
905    Quat. Sci. Rev., 28(25–26), 2582–2599, doi:https://doi.org/10.1016/j.quascirev.2009.05.014,

906    2009.

907    Morellón, M., Valero-Garcés, B., González-Sampériz, P., Vegas-Vilarrúbia, T., Rubio, E.,
908    Rieradevall, M., Delgado-Huertas, A., Mata, P., Romero, Ó., Engstrom, D. R., López-Vicente, M.,
909    Navas, A. and Soto, J.: Climate changes and human activities recorded in the sediments of Lake
910    Estanya (NE Spain) during the Medieval Warm Period and Little Ice Age, J. Paleolimnol., 46(3),
911    423–452, doi:10.1007/s10933-009-9346-3, 2011.

912    Moreno, A., Cacho, I., Canals, M., Grimalt, J. O., Sánchez-Goñi, M. F., Shackleton, N. and Sierro,
913    F. J.: Links between marine and atmospheric processes oscillating on a millennial time-scale. A
914    multi-proxy study of the last 50,000 yr from the Alboran Sea (Western Mediterranean Sea),
915    Quat. Sci. Rev., 24(14–15), 1623–1636, doi:https://doi.org/10.1016/j.quascirev.2004.06.018,
916    2005.

917    Moreno, A., Pérez, A., Frigola, J., Nieto-Moreno, V., Rodrigo-Gámiz, M., Martrat, B., González-
918    Sampériz, P., Morellón, M., Martín-Puertas, C., Corella, J. P., Belmonte, Á., Sancho, C., Cacho, I.,
919    Herrera, G., Canals, M., Grimalt, J. O., Jiménez-Espejo, F., Martínez-Ruiz, F., Vegas-Vilarrúbia, T.
920    and Valero-Garcés, B. L.: The Medieval Climate Anomaly in the Iberian Peninsula reconstructed
921    from marine and lake records, Quat. Sci. Rev., 43, 16–32,
922    doi:https://doi.org/10.1016/j.quascirev.2012.04.007, 2012.

923    Nestares, T. and Torres, T. de: Un nuevo sondeo de investigación paleoambiental del
924    Pleistoceno y Holoceno en la turbera del Padul (Granada, Andalucía). Geogaceta 23, 99-102.,
925    1997.

926    Olsen, J., Anderson, N. J. and Knudsen, M. F.: Variability of the North Atlantic Oscillation over
927    the past 5,200 years, Nat. Geosci, 5(11), 808–812, doi:10.1038/ngeo1589, 2012.

928    Ortiz, J. E., Torres, T., Delgado, A., Julià, R., Lucini, M., Llamas, F. J., Reyes, E., Soler, V. and Valle,
929    M.: The palaeoenvironmental and palaeohydrological evolution of Padul Peat Bog (Granada,
930    Spain) over one million years, from elemental, isotopic and molecular organic geochemical
931    proxies, Org. Geochem., 35(11–12), 1243–1260,
932    doi:https://doi.org/10.1016/j.orggeochem.2004.05.013, 2004.

933    Paillard, D., Labeyrie, L. and Yiou, P.: Macintosh Program performs time-series analysis, Eos
934    Trans. Am. Geophys. Union, 77(39), 379–379, doi:10.1029/96EO00259, 1996.

935    Pérez Raya, F. and López Nieto, J.: Vegetación acuática y helofítica de la depresión de Padul
936    (Granada), Acta Bot Malacit., 16(2), 373–389, 1991.

937    Pons, A. and Reille, M.: The holocene- and upper pleistocene pollen record from Padul
938    (Granada, Spain): A new study, Palaeogeogr. Palaeoclimatol. Palaeoecol., 66(3), 243–263,
939    doi:http://dx.doi.org/10.1016/0031-0182(88)90202-7, 1988.

940    Ramos-Román, M. J., Jiménez-Moreno, G., Anderson, R. S., García-Alix, A., Toney, J. L., Jiménez-
941    Espejo, F. J. and Carrión, J. S.: Centennial-scale vegetation and North Atlantic Oscillation

942   changes during the Late Holocene in the southern Iberia, Quat. Sci. Rev., 143, 84–95,
943   doi:https://doi.org/10.1016/j.quascirev.2016.05.007, 2016.

944   Reimer, P. J., Bard, E., Bayliss, A., Beck, J. W., Blackwell, P. G., Ramsey, C. B., Buck, C. E., Cheng,
945   H., Edwards, R. L., Friedrich, M., Grootes, P. M., Guilderson, T. P., Haflidason, H., Hajdas, I.,
946   Hatté, C., Heaton, T. J., Hoffmann, D. L., Hogg, A. G., Hughen, K. A., Kaiser, K. F., Kromer, B.,
947   Manning, S. W., Niu, M., Reimer, R. W., Richards, D. A., Scott, E. M., Southon, J. R., Staff, R. A.,
948   Turney, C. S. M. and van der Plicht, J.: IntCal13 and Marine13 Radiocarbon Age Calibration
949   Curves 0–50,000 Years cal BP, Radiocarbon, 55(4), 1869–1887, doi:10.2458/azu_js_rc.55.16947,
950   2013.

951   Riera, S., Wansard, G. and Julià, R.: 2000-year environmental history of a karstic lake in the
952   Mediterranean Pre-Pyrenees: the Estanya lakes (Spain), {CATENA}, 55(3), 293–324,
953   doi:https://doi.org/10.1016/S0341-8162(03)00107-3, 2004.

954   Riera, S., López-Sáez, J. A. and Julià, R.: Lake responses to historical land use changes in
955   northern Spain: The contribution of non-pollen palynomorphs in a multiproxy study, Rev.
956   Palaeobot. Palynol., 141(1–2), 127–137, doi:https://doi.org/10.1016/j.revpalbo.2006.03.014,
957   2006.

958   Rodrigo-Gámiz, M., Martínez-Ruiz, F., Rodríguez-Tovar, F. J., Jiménez-Espejo, F. J. and Pardo-
959   Igúzquiza, E.: Millennial- to centennial-scale climate periodicities and forcing mechanisms in the
960   westernmost Mediterranean for the past 20,000 yr, Quat. Res., 81(1), 78–93,
961   doi:https://doi.org/10.1016/j.yqres.2013.10.009, 2014.

962   Sanz de Galdeano, C., El Hamdouni, R. and Chacón, J.: Neotectónica de la fosa del Padul y del
963   Valle de Lecrín, Itiner. Geomorfológicos Por Andal. Orient. Publicacions Univ. Barc. Barc., 65–81,
964   1998.

965   Schulz, M. and Mudelsee, M.: REDFIT: estimating red-noise spectra directly from unevenly
966   spaced paleoclimatic time series, Comput. Geosci., 28(3), 421–426,
967   doi:https://doi.org/10.1016/S0098-3004(01)00044-9, 2002.

968   Sicre, M.-A., Jalali, B., Martrat, B., Schmidt, S., Bassetti, M.-A. and Kallel, N.: Sea surface
969   temperature variability in the North Western Mediterranean Sea (Gulf of Lion) during the
970   Common Era, Earth Planet. Sci. Lett., 456, 124–133,
971   doi:http://dx.doi.org/10.1016/j.epsl.2016.09.032, 2016.

972   Steinhilber, F., Beer, J. and Fröhlich, C.: Total solar irradiance during the Holocene, Geophys.
973   Res. Lett., 36(19), n/a–n/a, doi:10.1029/2009GL040142, 2009.

974   Trouet, V., Esper, J., Graham, N. E., Baker, A., Scourse, J. D. and Frank, D. C.: Persistent Positive
975   North Atlantic Oscillation Mode Dominated the Medieval Climate Anomaly, Science, 324(5923),
976   78, doi:10.1126/science.1166349, 2009.

977   Valle, F.: Mapa de series de vegetación de Andalucía 1: 400 000, Editorial Rueda., 2003.

978 Villegas Molina, F.: Laguna de Padul: Evolución geológico-histórica, Estud. Geográficos, 28(109),
979 561, 1967.

980 Zanchettin, D., Rubino, A., Traverso, P. and Tomasino, M.: Impact of variations in solar activity
981 on hydrological decadal patterns in northern Italy, J. Geophys. Res. Atmospheres, 113(D12),
982 n/a–n/a, doi:10.1029/2007JD009157, 2008.

983
984

985

986

987

988

989

990

991

992

993

994

995

996

997

998

999

1000

1001

1002

1003

1004

1005 **Figures and tables**
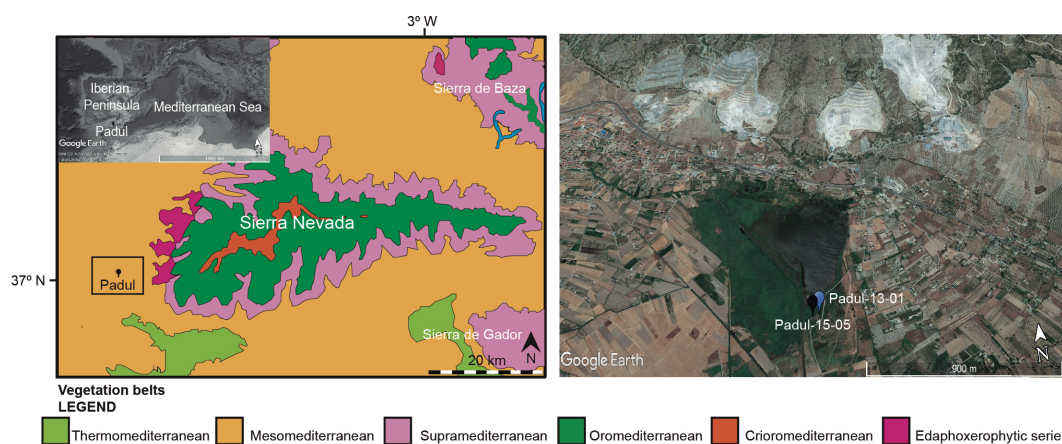
1006

1007 **Figure 1.** Location of Padul peat bog in Sierra Nevada National Park, southern Iberian
1008 Peninsula. Panel on the left is the map of the vegetation belts in the Sierra Nevada (Modified
1009 from REDIAM. Map of the vegetation series of Andalusia:
1010 http://laboratoriorediam.cica.es/VisorGenerico/?tipo=WMS&url=http://www.juntadeandalucia.e
1011 s/medioambiente/mapwms/REDIAM_Series_Vegetacion_Andalucia?). The inset map is the
1012 Google earth image of the Iberian Peninsula in the Mediterranean region. Panel on the right is
1013 the Google earth image (http://www.google.com/earth/index.html) of Padul peat bog area
1014 showing the coring locations.

1015

1016
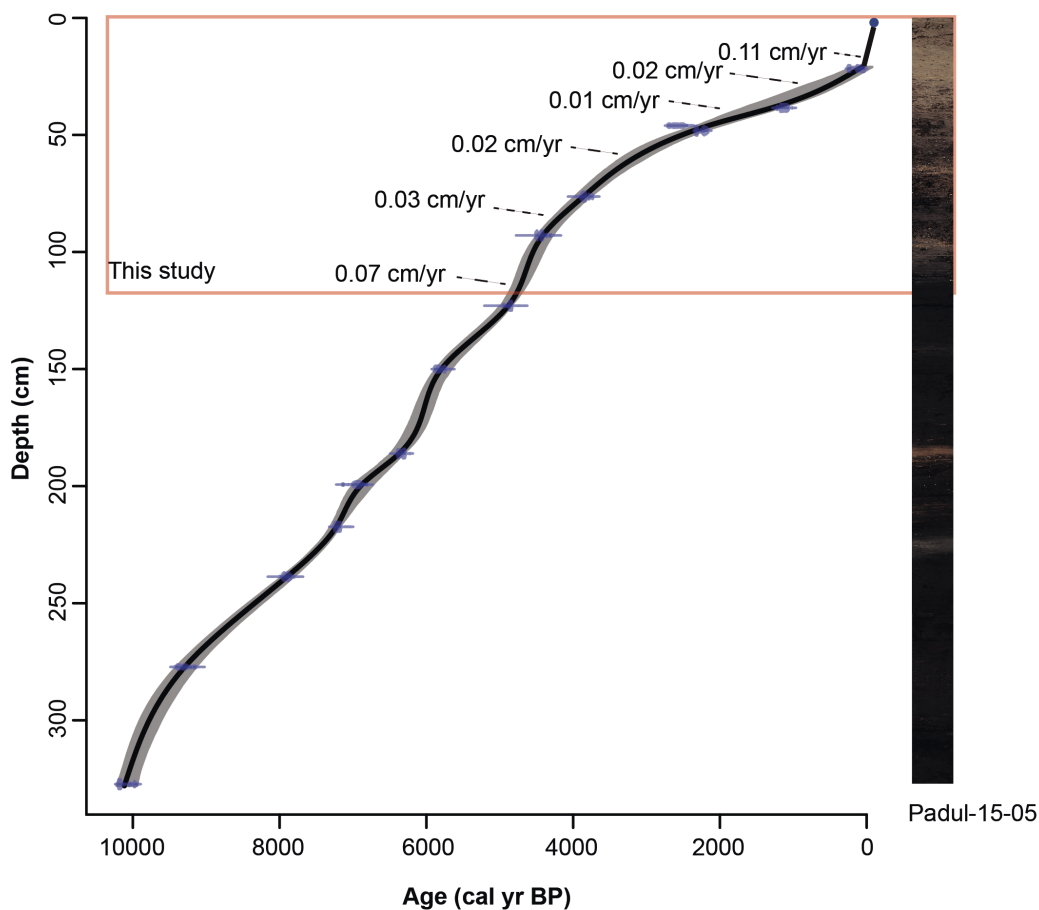
1017

**Figure 2.** Photo of the Padul-15-05 sediment core with the age-depth model showing the part of
the record that was studied here (red rectangle). The sediment accumulation rates (SAR) between
individual segments are marked. See the body of the text for the explanation of the age
reconstructions.

1018
1019
1020
1021

1022

1023
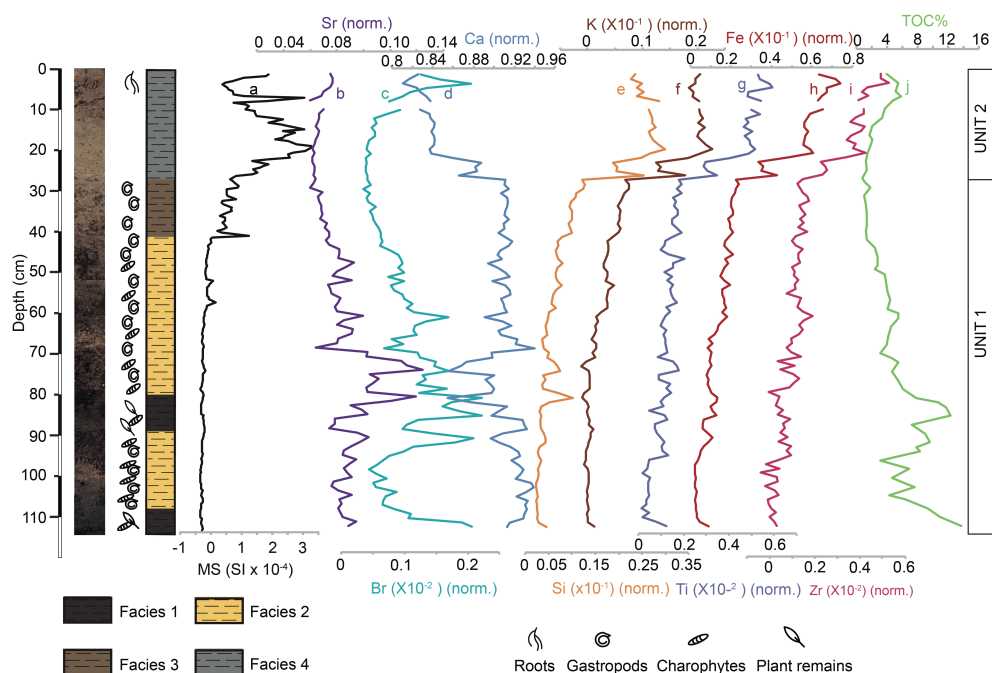
1024

**Figure 3.** Lithology, facies interpretation with paleontology, magnetic susceptibility (MS), and geochemical (X-ray fluorescence (XRF) and total organic carbon (TOC) data from the Padul-15-05 record. XRF elements are represented normalized by the total counts. (a) Magnetic susceptibility (MS; SI). (b) Strontium normalized (Sr; norm.). (c) Bromine norm. (Br; norm.). (d) Calcium normalized. (Ca; norm.). (e) Silica normalized (Si; norm.). (f) Potassium normalized (K; norm.). (g) Titanium normalized (Ti; norm.). (h) Iron normalized (Fe; norm.). (i) Zirconium normalized (Zr; norm.). (j) Total organic carbon (TOC %).

1032

1033

1034

1035

1036

1037

1038

1039
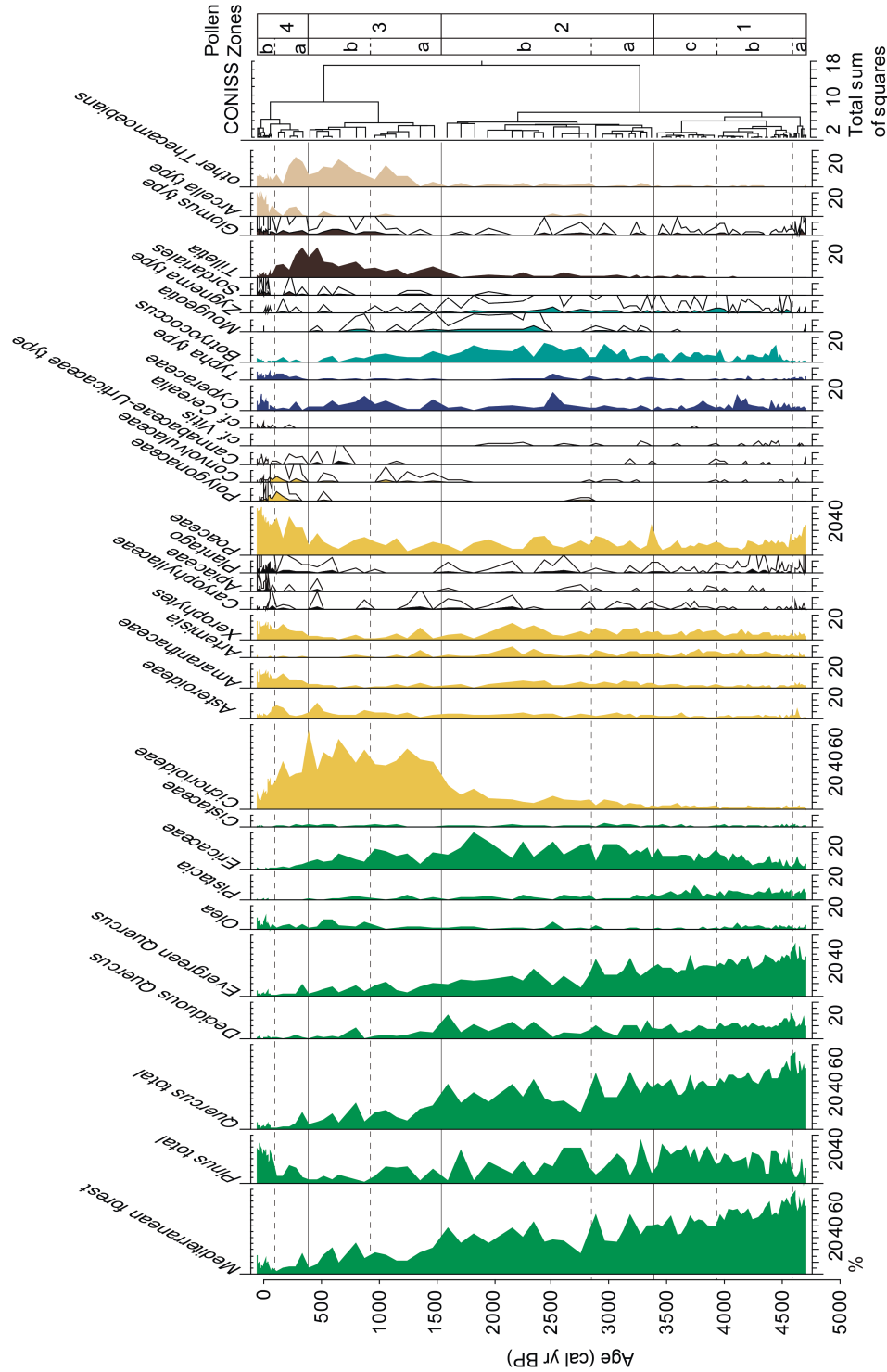
**Figure 4.** Percentages of selected pollen taxa and non-pollen palynomorphs (NPPs) from the Padul-15-05 record, represented with respect to terrestrial pollen sum. Silhouettes show 7-time exaggerations of pollen percentages. Pollen zonation is shown on the right. Tree and shrubs are showing in green, herbs and grasses in yellow, aquatics in dark blue, algae in blue, fungi in brown and thecamoebians in beige. The Mediterranean forest taxa is composed of *Quercus* total, *Olea*, *Phillyrea* and *Pistacia*. The xerophyte group includes *Artemisia*, *Ephedra*, and Amaranthaceae.
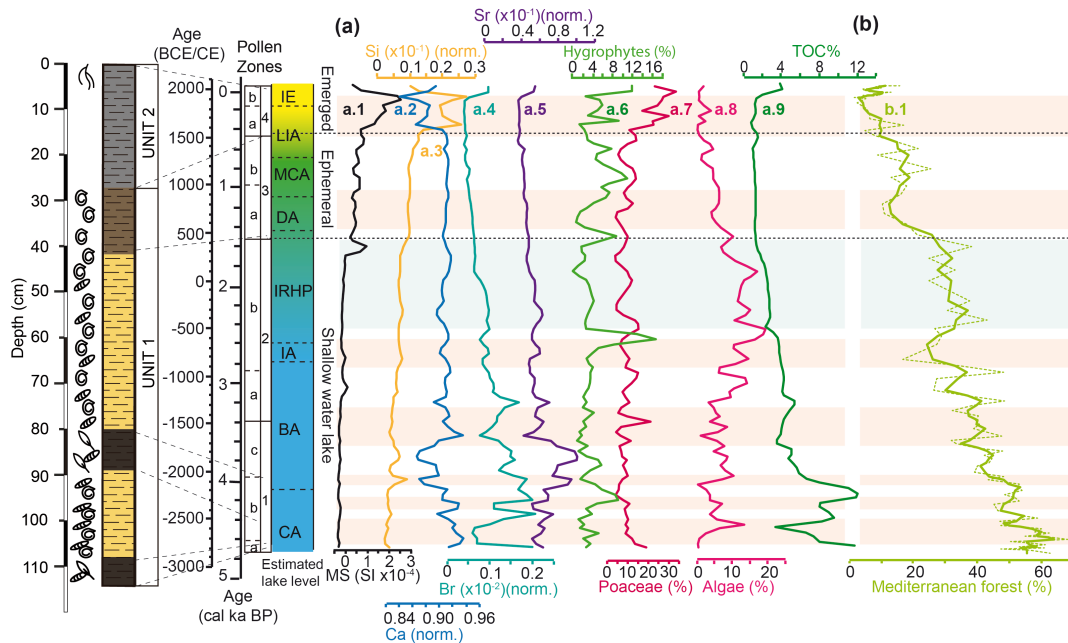
1059

**Figure 5.** Estimated lake level evolution and regional palynological component from the last ca. 4700 yr based on the synthesis of determinate proxies from the Padul-15-05 record: (a) Proxies used to estimate the water table evolution from the Padul-15-05 record (proxies were resampled at 50 yr (lineal interpolation) using Past software http://palaeo-electronica.org/2001_1/past/issue1_01.htm). [(a.1) Magnetic Susceptibility (MS) in SI; (a.2) Silica normalized (Si; norm.); (a.3) Calcium normalized (Ca; norm.); (a.4) Bromine normalized (Br; norm.) ; (a.5) Strontium normalized (Sr; norm.); (a.6) Hygrophytes (%); (a.7) Poaceae (%); (a.8) Algae (%) (a.9) Total organic carbon (TOC %) ] (b) Mediterranean forest taxa, with a smoothing of three-point in bold. Pink and blue shading indicates Holocene arid and humid regionally events, respectively. See the body of the text for the explanation of the lake level reconstruction. Mediterranean forest smoothing was made using Analyseries software (Paillard et al., 1996). CA = Copper Age; BA = Bronze Age; IA = Iron Age; IRHP = Iberian Roman Humid Period; DA = Dark Ages; MCA = Medieval Climate Anomaly; LIA = Little Ice Age; IE = Industrial Era.
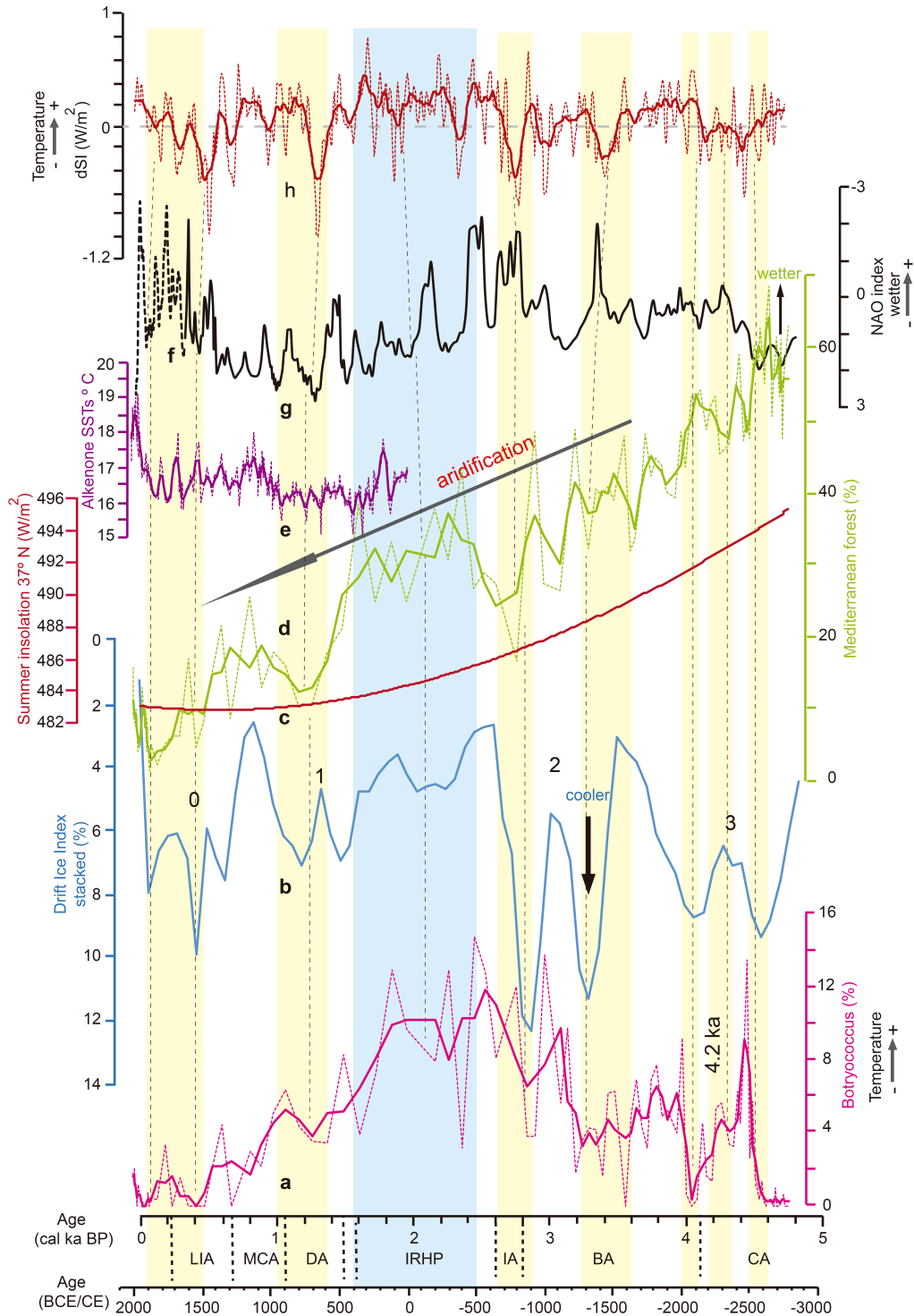
**Figure 6.** Comparison of the last ca. 4700 yr between different pollen taxa from the Padul-15-05 record, summer insolation for the Sierra Nevada latitude, eastern Mediterranean humidity and North Atlantic temperature. (a) *Botryococcus* from the Padul-15-05 record, with a smoothing of three-point in bold (this study). (b) Drift Ice Index (reversed) from the North Atlantic (Bond et al., 2001). (c) Summer insolation calculated for 37º N (Laskar et al., 2004). (d) Mediterranean forest taxa from the Padul-15-05 record, with a smoothing of three-point in bold (this study). (e) Alkenone-SSTs from the Gulf of Lion (Sicre et al., 2016), with a smoothing of four-point in bold. (f) North Atlantic Oscillation (NAO) index from a climate proxy reconstruction from Morocco and Scotland (Trouet et al., 2009). (g) North Atlantic Oscillation (NAO) index (reversed) from a climate proxy reconstruction from Greenland (Olsen et al., 2012). (h) Total solar irradiance reconstruction from cosmogenic radionuclide from a Greenland ice core (Steinhilber et al., 2009), with a smoothing of twenty-one-point in bold. Yellow and blue shading correspond with arid (and cold) and humid (and warm) periods, respectively. Grey dash lines show a tentative correlation between arid and cold conditions and the decrease in the Mediterranean forest and *Botryococcus*. Mediterranean forest, *Botryococcus* and solar irradiance smoothing was made using Analyseries software (Paillard et al., 1996), Alkenone-SSTs smoothing was made using Past software (http://palaeo-electronica.org/2001_1/past/issue1_01.htm). A linear r (Pearson) correlation was calculated between *Botryococcus* (detrended) and Drift Ice Index (Bond et al., 2001; r = -0.63; $p < 0.0001$; between ca. 4700 to 1500 cal ka BP – r=-0.48; $p < 0.0001$ between 4700 and -65 cal yr BP). Previously, the data were detrended (only in *Botryococcus*), resampled at 70-yr (linear interpolation) in order to obtain equally spaced time series and smoothed to three-point average. CA = Copper Age; BA = Bronze Age; IA = Iron Age; IRHP = Iberian Roman Humid Period; DA = Dark Ages; MCA = Medieval Climate Anomaly; LIA = Little Ice Age; IE = Industrial Era.
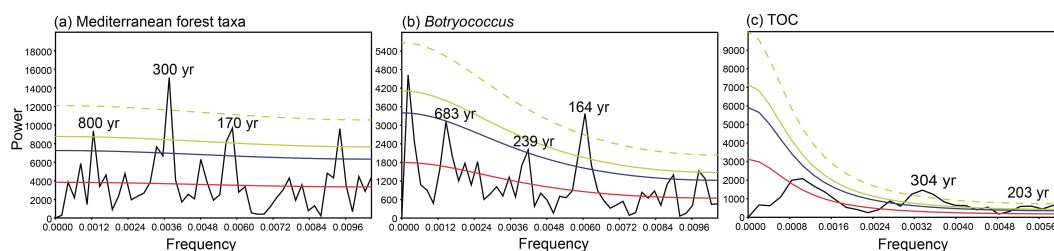
**Figure 7.** Spectral analysis of (a) Mediterranean forest taxa and (b) *Botryococcus* (mean sampling space = 47 yr) and (c) TOC (mean sampling space = 78 yr) from the Padul-15-05. The significant periodicities above confident level are shown. Confidence level 90 % (blue line), 95 % (green line), 99 % (green dash line) and AR (1) red noise (red line). Spectral analysis was made with Past software (http://palaeo- electronica.org/2001_1/past/issue1_01.htm).

1130    **Table 1.** Age data for Padul-15-05 record. All ages were calibrated using R-code package 'clam
1131    2.2' employing the calibration curve IntelCal 13 (Reimer et al., 2013) at 95 % of confident range.

1132    *Sample number assigned at radiocarbon laboratory

| Laboratory number | Core | Material | Depth (cm) | Age ($^{14}$C yr BP ± 1σ) | Calibrated age (cal yr BP) 95 % confidence interval | Median age (cal yr BP) |
|---|---|---|---|---|---|---|
| Reference ages | | | 0 | 2015CE | -65 | -65 |
| D-AMS 008531 | Padul-13-01 | Plant remains | 21.67 | 103 ± 24 | 23-264 | 127 |
| Poz-77568 | Padul-15-05 | Org. bulk sed. | 38.46 | 1205 ± 30 | 1014-1239 | 1130 |
| BETA-437233 | Padul-15-05 | Plant remains | 46.04 | 2480 ± 30 | 2385-2722 | 2577 |
| Poz-77569 | Padul-15-05 | Org. bulk sed. | 48.21 | 2255 ± 30 | 2158-2344 | 2251 |
| BETA-415830 | Padul-15-05 | Shell | 71.36 | 3910 ± 30 | 4248-4421 | 4343 |
| BETA-437234 | Padul-15-05 | Plant remains | 76.34 | 3550 ± 30 | 3722-3956 | 3838 |
| BETA-415831 | Padul-15-05 | Org. bulk sed. | 92.94 | 3960 ± 30 | 4297-4519 | 4431 |
| Poz-74344 | Padul-15-05 | Plant remains | 122.96 | 4295 ± 35 | 4827-4959 | 4871 |
| BETA-415832 | Padul-15-05 | Plant remains | 150.04 | 5050 ± 30 | 5728-5900 | 5814 |
| Poz-77571 | Padul-15-05 | Plant remains | 186.08 | 5530 ± 40 | 6281-6402 | 6341 |
| Poz-74345 | Padul-15-05 | Plant remains | 199.33 | 6080 ± 40 | 6797-7154 | 6935 |
| BETA-415833 | Padul-15-05 | Org. bulk sed. | 217.36 | 6270 ± 30 | 7162-7262 | 7212 |
| Poz-77572 | Padul-15-05 | Org. bulk sed. | 238.68 | 7080 ± 50 | 7797-7999 | 7910 |
| Poz-74347 | Padul-15-05 | Plant remains | 277.24 | 8290 ± 40 | 9138-9426 | 9293 |
| BETA-415834 | Padul-15-05 | Plant remains | 327.29 | 8960 ± 30 | 9932-10221 | 10107 |

1133

1134

1135

1136

**Table 2.** Linear r (Pearson) correlation between geochemical elements from the Padul-15-05 record. Statistical treatment was performed using the Past software (http://palaeo-electronica.org/2001_1/past/issue1_01.htm).

|  | Si | K | Ca | Ti | Fe | Zr | Br | Sr |
|---|---|---|---|---|---|---|---|---|
| **Si** |  | 8.30E-80 | 2.87E-34 | 7.47E-60 | 3.22E-60 | 5.29E-44 | 0.001152 | 7.79E-09 |
| **K** | 0.98612 |  | 7.07E-29 | 6.05E-60 | 8.20E-68 | 1.77E-51 | 0.00030317 | 5.38E-12 |
| **Ca** | -0.88096 | -0.84453 |  | 6.09E-42 | 5.81E-39 | 8.10E-34 | 0.35819 | 0.26613 |
| **Ti** | 0.96486 | 0.96501 | -0.91794 |  | 1.74E-74 | 1.12E-57 | 0.074223 | 8.88E-07 |
| **Fe** | 0.96546 | 0.97577 | -0.90527 | 0.98224 |  | 2.77E-66 | 0.051072 | 3.32E-08 |
| **Zr** | 0.92566 | 0.94789 | -0.8783 | 0.96109 | 0.97398 |  | 0.054274 | 7.16E-08 |
| **Br** | -0.31739 | -0.3506 | -0.091917 | -0.17755 | -0.19372 | -0.19116 |  | 4.03E-18 |
| **Sr** | -0.53347 | -0.61629 | 0.11113 | -0.46426 | -0.51386 | -0.50295 | 0.72852 |  |